Geobios 76 (2023) 53–74

Contents lists available at ScienceDirect

Geobios

journal homepage: www.elsevier.com/locate/geobio

Original article

A new rodent chronology for the late Neogene of Spain ☆

Jan A. van Dam [a,b,*], Pierre Mein [c], Miguel Garcés [d], Ronald T. van Balen [e,f], Marc Furió [b,g], Luis Alcalá [h]

[a] Department of Earth Sciences, Utrecht University, Vening Meinesz Building A, Princetonlaan 8a, 3584 CB Utrecht, the Netherlands
[b] Institut Català de Paleontologia Miquel Crusafont, c/ Columnes s/n Campus de la UAB 08193, Cerdanyola del Vallès, Barcelona, Spain
[c] A.R.P.A Université Lyon 1, Bâtiment Géode 69622, Villeurbanne Cedex, France
[d] Departament de Dinàmica de la Terra i de l'Oceà, Facultat de Ciències de la Terra, Geomodels Research Institute, Universitat de Barcelona, Barcelona, Spain
[e] Department of Earth Sciences, Vrije Universiteit Amsterdam, De Boelelaan 1085, 1081 HV Amsterdam, The Netherlands
[f] TNO-Geological Survey of the Netherlands, Princetonlaan 6, 3584 CB Utrecht, The Netherlands
[g] Serra Húnter Fellow, Universitat Autònoma de Barcelona, Geology Department, Cerdanyola del Vallès, 08193 Barcelona, Spain
[h] Parque de las Ciencias de Andalucía, Av. de la Ciencia, s/n, Granada 18006, Spain

ARTICLE INFO

Article history:
Received 10 March 2022
Accepted 11 January 2023
Available online 23 January 2023

Keywords:
Miocene
Pliocene
Spain
Rodentia
Biostratigraphy
Geochronology

ABSTRACT

The number of late Neogene Spanish micromammal-containing continental sections with a correlation to the Geomagnetic Time Scale is steadily growing. Nonetheless, well-calibrated sections with dense micromammal records are still rare, biostratigraphic correlations between basins are not straightforward, and ages of uncalibrated sites are poorly constrained. Here, we aim at improving the chronology of Iberian micromammal sections and sites for the interval 8.5–2 Ma by: (*i*) analyzing qualitative and quantitative similarities between rodent assemblages and turnover in the different basins, (*ii*) formulating a system of fifteen Iberian assemblage biozones, and (*iii*) constraining the ages of zone boundaries, assuming isochroneity across basins. Age uncertainty ranges for most known Iberian micromammal sites are obtained by combining regional biozone boundary ages with local magnetostratigraphic records, sedimentation rates and/or evolutionary rates. In addition, our results include new, integrated stratigraphic records from the Jumilla-La Celia and Teruel Basins, which are used to constrain the thus far poorly dated interval covering the latest Tortonian and earliest Messinian (8–7 Ma).

1. Introduction

The use of paleomagnetism for dating Spanish continental sediments dates back a long time (Dijksman, 1977). It was not until the nineteen-nineties, however, that mammal-containing sections across the Iberian Peninsula started to be sampled in a systematic way (Krijgsman et al., 1994, 1996; Garcés et al., 1996, 1998; Agustí et al., 2001). Currently, the magnetostratigraphic framework for the late Neogene and its correlation to the Geomagnetic Polarity Time Scale (GPTS) includes many sections, of which the most important ones are situated in the Teruel Basin (La Gloria – Búnker de Valdecebro, Villalba Alta, Orrios, Escorihuela, Gea, Concud Estación), Cabriel Basin (Cabriel, Venta del Moro, La Bullana, Fuente del Viso), Júcar Basin (Valdeganga), Fortuna Basin (Chorrico, Sifón de Librilla), and Guadix-Baza Basins (Galera, Zújar, Gorafe) (Krijgsman et al., 1996; Garcés et al., 1997, 1998,1999; Opdyke et al., 1997; Oms et al., 1999; van Dam et al., 2001; Agustí et al., 2006a; Piñero et al., 2018; see Fig. 1 for the location of basins).

Even though almost every subinterval is covered magnetostratigraphically by one or more sections, many late Neogene mammal sites of the Iberian Peninsula still lack accurate age estimates. The main reason for this is the absence of a regional (Iberian) biostratigraphic framework with well-dated boundaries. Although a lack of resolution is plaguing both the macro- and micromammal record, the density of micromammal localities and specimens is much higher, making this group the most suitable for biostratigraphy. Within micromammals, rodents have traditionally been used for the definition of biozones because of their abundance and rapid evolution. The revision in this study thus embodies the integration of local (basin-scale) rodent-based biozonations into a regional-scale, Iberian stratigraphic framework. This framework, in turn, will be used to make chronological inferences for most Iberian micromammal sites by combining ages of regional zone boundaries with local sedimentation and/or evolutionary rates.

The use of regional biozone boundaries as age calibration points for local stratigraphic interpolation requires these boundaries to be isochronous. Although time equivalence of biozones is suggested

☆ Corresponding editor: Gilles Escarguel.

* Corresponding author at: Department of Earth Sciences, Utrecht University, Vening Meinesz Building A, Princetonlaan 8a, 3584 CB Utrecht, the Netherlands.
E-mail address: j.a.vandam@uu.nl (J.A. van Dam).

https://doi.org/10.1016/j.geobios.2023.01.001
0016-6995/

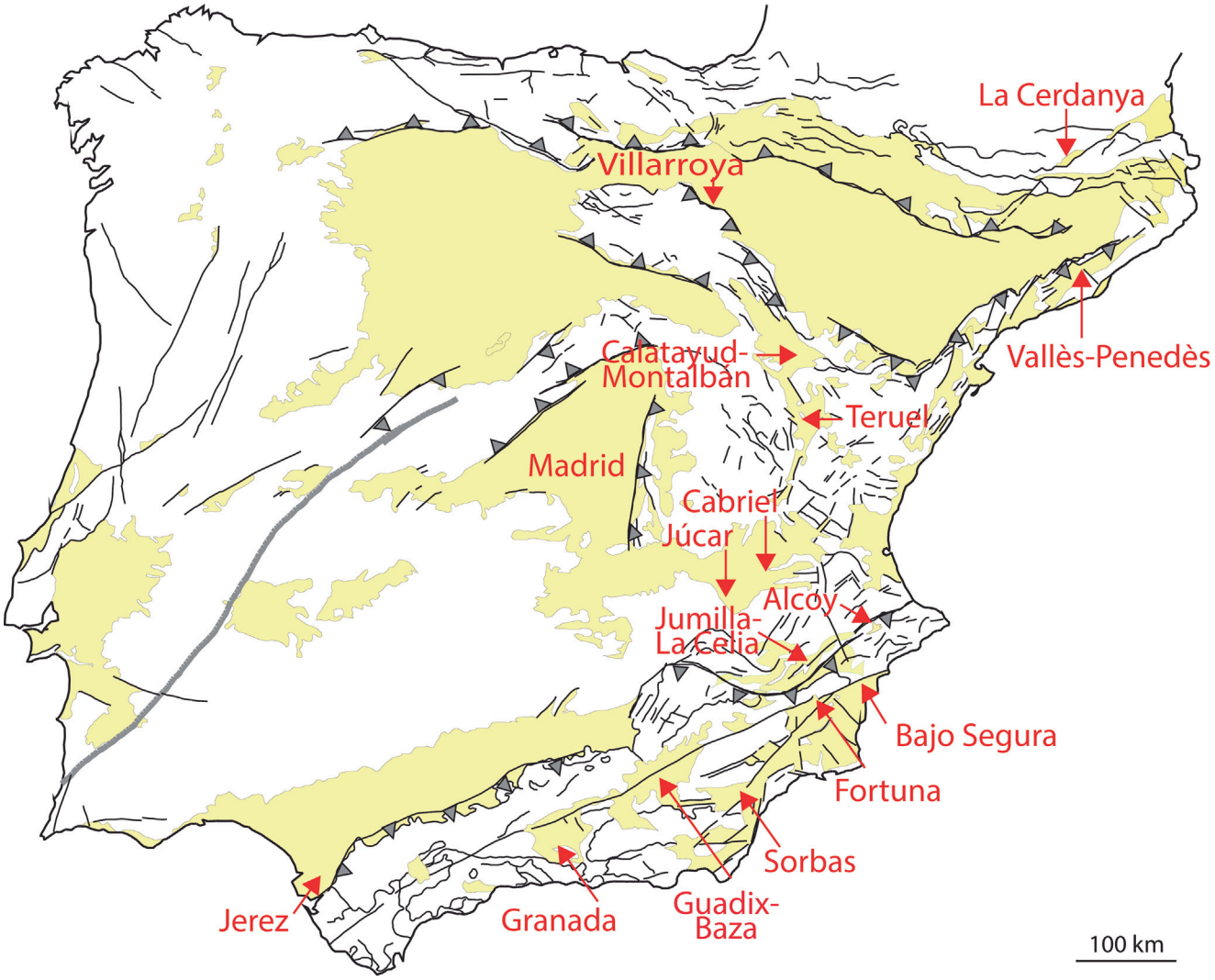

Fig. 1. Map of the Iberian Peninsula with Cenozoic basins in yellow. Names correspond to basins used in this study.

by the strong parallels between the local biozonation systems currently in use in terms of numbers and names of zones (Fig. 2), we prefer to go one step further and perform actual computations of faunal similarity, both in terms of numbers of species and relative abundances. Specifically, we will draw upon 'shared turnover' (i.e., between-basin shared species last and first occurrences) in order to characterize the magnitude and geographical extent of potential 'events' underlying community change at biozone boundaries.

The latest Tortonian to earliest Messinian (8–7 Ma) is chronologically one of the most poorly constrained late Neogene intervals on the Iberian Peninsula. In this paper, we will fill this gap by including new faunal, magnetostratigraphic and cyclostratigraphic data from the Jumilla – La Celia and Teruel Basins.

2. Stratigraphic background

2.1. Biostratigraphy

Existing Iberian latest Miocene and Pliocene local biozonation schemes have a very similar structure, with approximately the same number of zones often carrying the same names and largely containing the same dominant species. As a result, local zone sequences have been mutually correlated to each other in a routine fashion (Mein et al., 1990; van Dam et al., 2001; García-Alix et al., 2008a; Minwer-Barakat et al., 2012; Mansino et al., 2017; Piñero et al., 2018; Fig. 2).

Between-region faunal similarities across Spain were already observed in the nineteen-eighties (Mein et al., 1983; Godoy et al., 1983; Adrover, 1986), although at that time most biostratigraphic units were considered to have a large geographic domain, even up to the scale of the entire European continent. Accordingly, the just erected system of Neogene European Mammal units (MN1-17; Mein, 1989; Agustí et al., 2001, Hilgen et al., 2012) was instantly adopted as the starting point for further subdivision (e.g., 'MN15a/b', 'MN16a/b'). However, with an increasing number of magnetostratigraphic studies appearing, first and last appearances of species and genera not seldomly turned out could be diachronous at the continental scale, effectively reducing the domain of isochroneity to restricted bioprovinces only (van Dam, 2003; van der Meulen et al., 2012). As strong diachrony is expected to correlate to low faunal similarity (the common cause being a barrier of some kind), continents such as Europe are expected to be characterized by strong faunal heterogeneity. Indeed, the overlap between late Neogene Iberian and Central European faunas (Daxner-Höck, 1980; Dahlmann, 2001; Franzen et al., 2013) typi-

marine Age (sub-epoch)	MN unit (continental sub-age)	Teruel Basin (Mein et al., 1990; van Dam et al., 2001; this paper)	Bajo Segura Basin (Martín-Suárez and Freudenthal, 1998)	Alcoy Basin (Mansino et al., 2017)	Granada Basin (García-Alix et al., 2008a)	Guadix-Baza Basin (Agustí, 1990; Oms et al., 2000; Minwer-Barakat et al., 2012; Piñero et al., 2018; Piñero and Verzi, 2020)	proposed Iberian zone (assemblage zone, this paper)
Gelacian (early Pleistoc.)	**MN17** (late Villanyian)					***Mimomys* cf. *reidi* Range Zone**	***Mimomys realensis*** (Ib-N17b)
						***Mimomys medasensis* Range Zone**	***Mimomys medasensis*** (Ib-N17a)
Piacenzian (late Pliocene)	**MN16** (early Villanyian)	***Kislangia ischus* Range Zone** (O4) (= 'Zone of *Kislangia* ')				***Kislangia ischus* Range Zone**	***Kislangia ischus*** (Ib-N16b)
		***Mimomys hassiacus - Kislangia ischus* Interval Zone** (O3) (= 'Zone *M.gracilis* + *M.hajnackensis* ') FO *M.hassiacus* - FO *Kislangia*				***Mimomys polonicus* Range Zone**	***Mimomys hassiacus*** (Ib-N16a)
						***Mimomys hassiacus* Range Zone**	
	MN15 (late Ruscinian) (=late Alfambrian)	***Dolomys* Range Zone** (O2) (= 'Zone of *Dolomys* ')			***Stephanomys donnezani* Assemblage Zone** *Stephanomys donnezani*, *Trilophomys* sp., Arvicolinae indet., *Castillomys* cf. *crusafonti*	***Dolomys adroveri* Range Zone**	***Dolomys adroveri*** (Ib-N15b)
		***Mimomys - Dolomys* Interval Zone** (O1) (= 'Zone of *Mimomys* archaique') FO *Mimomys* - FO *Dolomys*				***Mimomys davakosi* Interval Zone** FO *M. davakosi* - FO *D. adroveri*	***Mimomys davakosi*** (Ib-N15a)
Zanclean (early Pliocene)	**MN14** (early Ruscinian) (=early Alfambrian)	***Trilophomys - Mimomys* Interval Zone** (= 'Zone of Trilophomys') FO *Trilophomys* - FO *Mimomys*		***Trilophomys* Assemblage Zone** *Apocricetus barrieri, S. cordii, C. gracilis, Apodemus gorafensis, Paraethomys meini, P. baeticus, Trilophomys*		***Trilophomys* Interval Zone** FO *Trilophomys* - FO *Mimomys davakosi*	***Trilophomys castroi*** (Ib-N14c)
		***Paraethomys baeticus - Trilophomys* Interval Zone** (N2) (= 'Zone 2 *Paraethomys* + *Promimomys* ') FO *P. baeticus* - FO *Trilophomys*		***Paraethomys baeticus* Interval Zone** FO *P. baeticus* - FO *Trilophomys*	***Paraethomys baeticus* Range Zone**	***Paraethomys baeticus* Range Zone**	***Paraethomys baeticus*** (Ib-N14b)
		***Celadensia* Range Zone** (N1) (= 'Zone of *Celadensia* ')		***Apocricetus barrierei* Interval Zone** FO *Apocricetus barrierei* - FO *Paraethomys baeticus*	***Apocricetus barrierei* Interval Zone** FO *Apocricetus barrierei* - FO *Paraethomys baeticus*	***Apocricetus barrierei* Interval Zone** FO *Apocricetus barrierei* - FO *Paraethomys baeticus*	***Apocricetus barrierei*** (Ib-N14a)
Messinian (late late Miocene)	**MN13** (late Turolian) (=Ventian)	***Paraethomys meini - Celadensia* Interval Zone** (M3) FO *Paraethomys meini* - FO *Celadensia*	***Paraethomys* Concurrent-range Zone** *Paraethomys meini, Apodemus gudrunae*	***Paraethomys meini* Interval Zone** FO *Paraethomys meini* - FO *Apocricetus barrieri*	***Paraethomys meini* Interval Zone** FO *Paraethomys meini* - FO *Apocricetus barrieri*	***Apodemus gudrunae - Apocricetus alberti* Concurrent-Range Zone** *Apodemus gudrunae, Apocricetus alberti*	***Paraethomys meini*** (Ib-N13c)
		***Castromys inflatus - Paraethomys meini* Interval Zone** (M2) LO *Castromys inflatus* - FO *P. meini*			***Apocricetus alberti* Interval Zone** FO *A. alberti* - FO *Paraethomys*		***Apocricetus alberti*** (Ib-N13b)
		***Castromys inflatus* Range Zone** (M1)	***Castromys inflatus* Interval Zone** FO *Stephanomys ramblensis* - FO *Paraethomys meini*		***Occitanomys adroveri - O. alcalai* Concurrent-range Zone** *Occitanomys adroveri, O. alcalai*		***Castromys inflatus*** (Ib-N13a)
	MN12 (middle Turolian)	***Parapodemus barbarae - Castromys inflatus* Interval Zone** (L2) LO *Parapodemus barbarae* - FO *Castromys inflatus*	***Parapodemus meini* Interval Zone** FO *Parapodemus meini* - FO *Stephanomys ramblensis*		***Castromys littoralis* Range Zone**		***Parapodemus meini*** (Ib-N12b)
		***Parapodemus barbarae* Range Zone** (L1)	***Huerzelerimys turoliensis* Concurrent-range Zone** *Huerzelerimys turoliensis, Parapodemus barbarae*				***Huerzelerimys turoliensis*** (Ib-N12a)
late Tortonian (early-middle late Miocene)	**MN11** (early Turolian)	***Huerzelerimys vireti* Range Zone** (K)	***Occitanomys sondaari* Concurrent-range Zone** *Occitanomys sondaari*				***Huerzelerimys vireti*** (Ib-N11)

Fig. 2. State-of-the-art correlation table between local Iberian biozones, newly proposed Iberian biozones, European-scale MN units, and Stages/Ages. Definitions of local zones are given implicitly (Range Zones), by first and last occurrences (FO/LO, for Concurrent-Range Zones) or by species lists (for Assemblage Zones). MN Zones are defined faunistically and not stratigraphically (Hilgen et al., 2012).

cally consists of two or three species only. Even examples of zero species overlap are known, e.g., between latest Miocene faunas of the Western and Eastern Mediterranean; Schmidt-Kittler, 1995; van Dam, 2003).

The similarities in number of zones and names between local Spanish latest Miocene to earliest Pleistocene zonation schemes (Fig. 2) suggest that the Iberian Peninsula largely functioned as a single bioprovince during this period. As can be seen in the table, the number of zones within approximately correlative larger stratigraphic units such as (sub-)Stages or MN units is mostly the same. For example, MN11 and MN12 (lower and middle Turolian) are covered by one and two local zones, respectively, in both the Bajo Segura and Teruel Basins. Similarly, MN13 (upper Turolian or 'Ventian') is covered by three named zones in the Teruel and Granada Basin, and MN14 (lower Ruscinian) by three zones in the Teruel, Alcoy, and Guadix-Baza Basins (with MN14 defined faunistically and not stratigraphically; in the latter case it is shortened, because of the early entry of the MN15-defining species *Mimomys davakosi* in Greece (Hilgen et al., 2012; Hordijk and de Bruijn, 2009)). Finally, MN15 and MN16 are covered by two zones in both the Teruel and Guadix-Baza Basins. 'Mismatches' can be explained by the occurrence of barren intervals: the lack of a 'middle MN13' zone in the Bajo Segura basin (Martín-Suárez and Freudenthal, 1998: between Crevillente 31 and Crevillente 6) and the lack of an 'upper MN14′ interval in the Granada Basin (part of the 'Barren Interval 2' of García-Alix et al., 2008a). Only two locally defined zones cannot be straightforwardly correlated to other basins: the *Stephanomys donnezani* Assemblage Zone in the Granada Basin and the *Mimomys polonicus* Zone in the Guadix-Baza Basin. The first of these, which is represented by the sites of the Barranco del Blas (García-Alix et al., 2007), is a 'floating' zone separated from the next older zone by the above-mentioned barren interval and (besides unidentifiable arvicoline material) containing species that can be correlated to either MN15 or MN16 (e.g., *Ruscinomys* cf. *europaeus*, *Stephanomys donnezani*, *Castillomys crusafonti*). The *Mimomys polonicus* Zone is a short zone between the *Mimomys hassiacus* and *Kislangia ischus* Zones, of which the definition is based on a single and thus far poorly documented occurrence of *M. polonicus* in Zújar 10 (Piñero et al., 2018). Also given the prospect of synonymizing *M. polonicus* with *M. hassiacus* (Tesakov, 1998), the usefulness of this zone for overall Iberian biostratigraphy is doubtful.

Time equivalence of zones is also suggested by the use of identical zone names (Fig. 2), reflecting pan-Iberian occurrences of characteristic species. Examples are (fractions refer to the number of basins): *Huerzelerimys turoliensis* (MN12: 2/2), *Castromys inflatus* (MN13: 2/3), *Paraethomys meini* (MN13: 3/5, *Apocricetus barrieri* (MN13: 3/4), *Paraethomys baeticus* (MN14: 4/4), *Trilophomys* (MN14: 3/4), *Dolomys* (*adroveri*) (MN15: 2/3), *Kislangia* (*ischus*) (MN16: 2/3). The use of different names is sometimes semantic: for instance, the Zone of '*Mimomys* archaïque' (MN15 Teruel Basin) effectively applies to *M. davakosi*, as used in the names of corresponding zones. In still other cases, the use of different names used is only a matter of coincidence, with the same combinations of species present in time-equivalent zones.

Although the concept of a single Iberian province with homogeneous biostratigraphic units separated by isochronous zone boundaries is suggested by Fig. 2, actual quantitative analyses of faunal similarity and shared turnover are thus far lacking. It is one of the gaps we aim to fill in this work.

2.2. Tortonian-Messinian transitional interval

Until now, the Tortonian-Messinian transition interval (which is approximately time-equivalent to the continental middle-upper Turolian, or Turolian-Ventian transition; Morales et al., 2013) is poorly constrained in continental Spanish records. Either a faunal gap is present despite a well-documented magnetostratigraphic record (e.g., Fortuna Basin; Agustí et al., 2006a; Garcés et al., 1998; Piñero and Agustí, 2019) a magnetostratigraphic gap exists despite a rich and well-documented faunal record (e.g., Bajo Segura Basins and Teruel Basins; Martín-Suárez and Freudenthal, 1998; van Dam et al., 2001). The correlation problems pertaining to this interval are reflected in a large age uncertainty for the approximately correlative MN12/13 transition (7.4–6.8 Ma; Hilgen et al., 2012).

The new magnetostratigraphic and cyclostratigraphic results for the late Tortonian and early Messinian that will be presented in this work are based on sections in the Teruel and Jumilla-La Celia Basins (Figs. 1–3). The Teruel Basin is a half-graben situated within the Iberian Chain and contains a fairly complete succession of Late Miocene and Pliocene continental sediments (Anadón et al., 1990; Alonso-Zarza and Calvo, 2000; Ezquerro et al., 2020). The basin is well-known for its rich mammal record (van de Weerd, 1976; Adrover, 1986; Mein et al., 1990; Alcalá, 1994; van Dam et al., 2001; Alcalá et al., 2018). A significant part of the record is constrained magnetostratigraphically (Krijgsman et al., 1996; Opdyke et al., 1997; Garcés et al., 1999). Locally, the age accuracy of mammal sites has been further increased using orbitally forced lithological alternations (early Late Miocene; Abdul Aziz et al., 2004; Abels et al., 2009b).

The Jumilla-La Celia basin is a small basin situated along the Jumilla Fault Zone (JFZ) in the external part of the eastern Betic Cordillera (van Balen et al., 2015). The basin is known for its late Neogene volcanics aged 7.6–7.2 Ma (7.8–6.9 Ma with error bars included) based on K-Ar data (Nobel et al., 1981). A re-interpretation of micromammal data (sites La Celia and Los Gargantones; van Dam et al., 2014) indicates a consistent MN12-correlative age (between 7.6 and ~7 Ma; Hilgen et al., 2012).

3. Material and methods

3.1. Sampled sections Tortonian-Messinian transition

Three parallel sections were studied near the village of Concud in the Teruel Basin (Fig. 3). These sections contain or are close to the well-known micromammal sites of Concud Cerro de la Garita (CC), Concud Barranco de las Calaveras (CCL) and Las Pedrizas (Concud 2 and 3; CC2, CC3) as previously described (van de Weerd, 1976; Alcalá, 1994) (Fig. 4(A–E)). The Concud Cerro de la Garita (CCCG) section consists of a lower alluvial part consisting of red mudstones and an upper shallow lacustrine part dominated by limestones and marls (Fig. 4(D)). The alluvial part was sampled paleomagnetically. Although the magnetic signal in the Las Pedrizas (CCLP) was too weak to perform a reliable magnetostratigraphic study, the regular bedding pattern of this section and of the Barranco de las Calaveras (CCBC) section could be interpreted cyclostratigraphically and was used as an additional tool in dating mammal sites. Seven hand samples from the CCLP section were subjected to X-ray diffraction (XRD) to check the mineral composition of the sediments. In addition, thin sections were prepared from these samples to study microscopic features.

The two parallel sections of La Celia (JCLC) and Los Barracones (JCBA) in the Jumilla – La Celia Basin were sampled paleomagnetically. These two sections, which are separated geographically by 1–1.5 km, reveal a rapid lateral sedimentary facies change (Fig. 4 (F–H)). Whereas the JCLC section dominantly consists of conglomerates, reddish mudstones, silts, and fine sands, pointing to a proximal sedimentation regime (debris flows; van Balen et al., 2015), the JCBA section mainly contains reddish to greenish mudstones and gypsum, indicating distal alluvial to shallow lacustrine conditions.

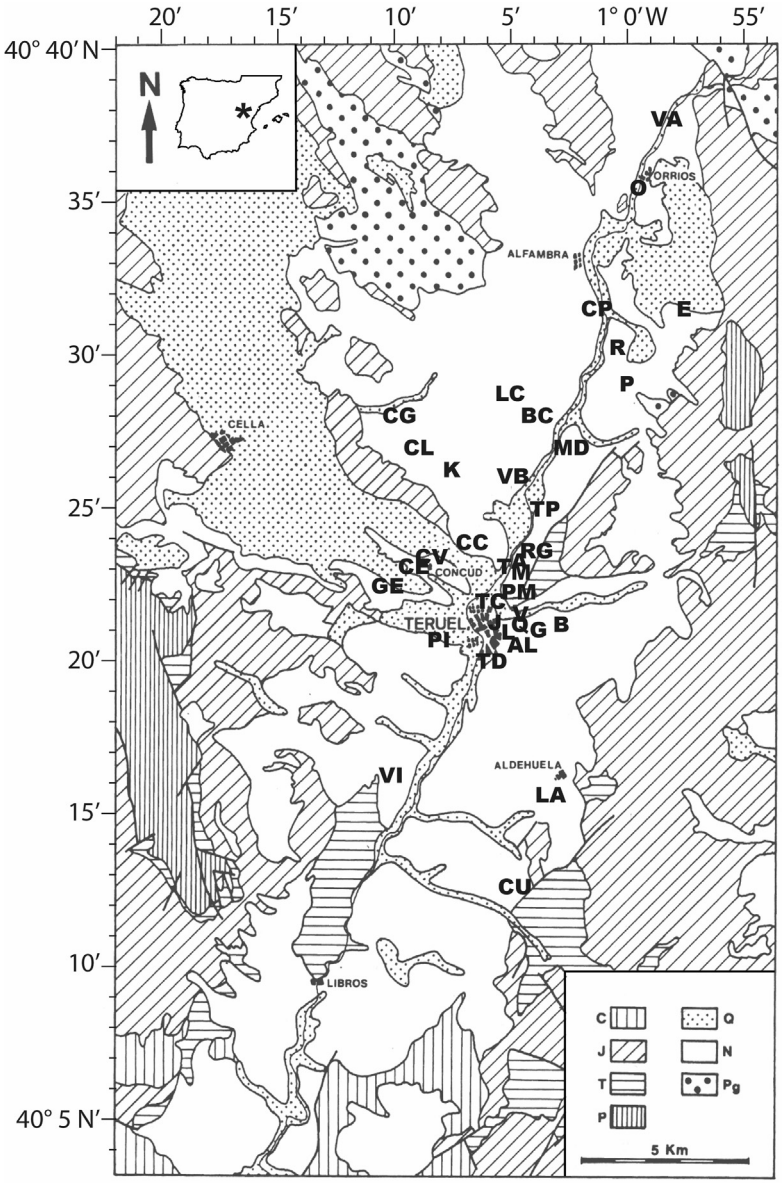

Fig. 3. Geological map of the central part of the Teruel Basin with fossil sites. CP: El Capón; E: Escorihuela; O: Orrios; P: Peralejos; MD: Modorras; VA: Villalba Alta and Villalba Alta Río; LC: Lomas de Casares; BC: Barranco de Cuevas; R: La Roma; VB: Villalba Baja; CC: Concud Cerro de la Garita, Barranco de las Calaveras and Las Pedrizas; CG: Cerro Gordo; CL: Celadas; K: Las Casiones; TP: Tortajada Pueblo; RG: El Regajo; A: Alfambra; T: Tortajada; M: Masada del Valle and Masada Ruea, PM: Puente Minero; TC: Teruel Transformadores and Teruel Cementerio; V: Valdecebro; Q: El Arquillo; J: Teruel Judería; LM: Los Mansuetos; AL: Aljezar B; G: La Gloria and Los Aguanaces; B: El Búnker (de Valdecebro); TD: Teruel Desvío; PI: Poblado Ibérico; GE: Gea (=La Guea); CE: Concud Estación; CV: Concud Village; LA: La Calera; VI: Villastar; CU: Cubla. Abbreviations: P, Paleozoic; T, Triassic; J, Jurassic; C, Cretaceous; Pg, Paleogene; N, Neogene; Q, Quaternary.

3.2. Magnetostratigraphy

An average sampling resolution of about 1 site/meter was applied and samples were drilled in situ and oriented with a magnetic compass mounted on a clinometer device. A total of 130 samples were processed in the laboratory, sharing a similar lithology consisting of red clay, silt and silty sandstone.

Paleomagnetic analysis consisted of stepwise thermal demagnetization of the natural remanent magnetization (NRM) of one sample per site, in order to isolate the most stable characteristic remanent magnetization (ChRM). The remanence vector was measured in the 2G-SRM750 superconducting rock-magnetometer of the laboratory of paleomagnetism of the CCiTUB (University Barcelona-CSIC). Measurement of the magnetic susceptibility followed each demagnetization step in order to monitor chemical changes of the magnetic mineralogy upon heating. ChRM directions were picked by visual inspection of Zijderveld plots and calculated by principal component analysis. In order to interpret the polarity of the samples, the latitude of the virtual geomagnetic pole (VGP) was calculated from each ChRM direction, and positive (negative) VGP latitudes were interpreted as normal (reversed) polarity.

3.3. Micromammal paleontology

One larger (CG5, n = 374) and four smaller micromammal localities (CG1,2,4,6,7, 40°24′2″N, 1°8′52″W, total n = 43) were sampled above and below the classic macromammal site of Concud Cerro de la Garita (CCCG; Fig. 4(E)) in the Teruel Basin. A previously described small micromammal sample from this classic level (code

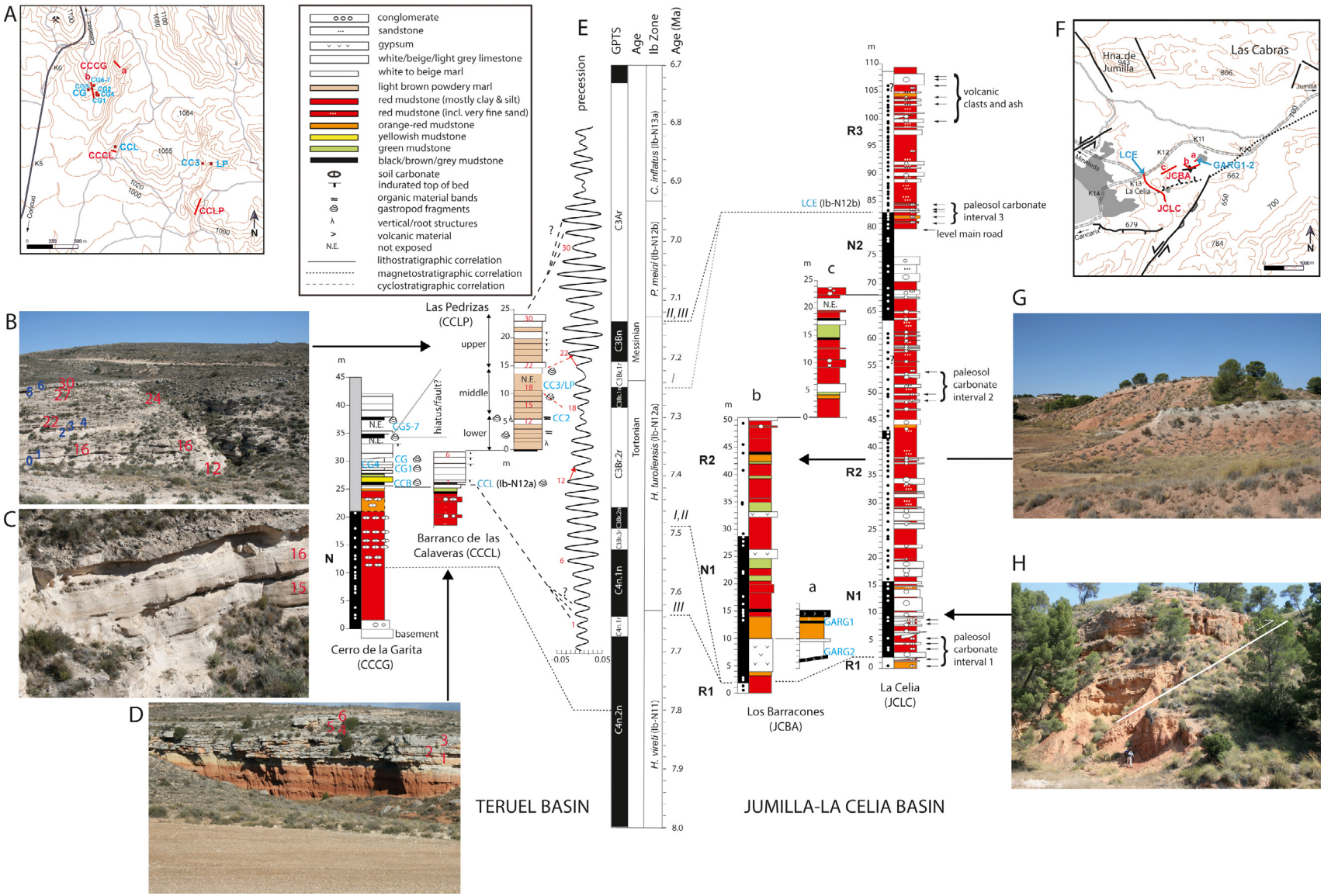

Fig. 4. Chronological interpretation of middle Turolian (latest Tortonian – earliest Messinian) sediments in the Teruel and Jumilla-La Celia Basins. **A**. Local map with approximate section paths (in red) and sites (in blue) near Concud; K: kilometer mark along main road. **B**. Cyclically deposited beds in the Las Pedrizas (CCLP) section; cycle numbers in red, rock samples in blue. **C**. Internally laminated beds in the CCLP section, cycle numbers in red. **D**. Cyclically deposited beds in the Barranco de las Calaveras (CCBC) section; cycle numbers in red. **E**. Studied sections and correlations to the Geological Time Scale (Raffi et al., 2020). **F**. Local map with approximate section paths (in red) and sites (in blue) near La Celia; K: kilometer mark along main road; dark grey area: volcanic deposits; light grey area: diapir. **G**. Mudstones, gypsum and carbonate deposits in Los Barracones (JCBA) section. **H**. Conglomerates and mudstones in basal part La Celia (JCLC) section, with local fault indicated.

CC in van de Weerd, 1976) was extended (total n = 467, new material coded CG). Furthermore, two new sites (La Roma 5A and 5B, R5A-B; 40°30′8″N, 1°0′40″W, n = 225 and 425, respectively) were sampled north of the village of Peralejos about 500 m east of the macro- and micromammal site La Roma 2 (Zone J3; Alcalá, 1994; Alcalá et al., 2005; Fig. 3). The stratigraphic context of both sites is somewhat obscured by the local deposition of Quaternary gravels and recent valley fill. Bed tracing suggests that R5A and B belong to a highly condensed (∼10 m thick) interval bracketed by basal Zone L (Peralejos D) and Zone M1-2 faunas (El Capón 2) (faunal information in van Dam et al., 2001). Finally, a small collection (Tortajada Pueblo, TOP, 40°24′30″N, 1°4′00″W; n = 6; Fig. 3) was sampled at the transition between carbonate/marls (Alfambra Fm.) and gypsum (Tortajada Fm.) near the village of Tortajada (formation names after van de Weerd (1976)). All newly sampled rodent teeth were measured using the methods as described by van de Weerd (1976) except for Gliridae, which were measured according to Daams (1983). The newly sampled material is housed in the Museo Aragonés de Paleontología (Teruel).

Besides a summary of the newly sampled Late Miocene material, we also include unpublished measurement statistics of previously described Late Miocene localities (Besems and van de Weerd, 1983; van Dam, 1997; van Dam et al., 2001) and faunal lists for Pliocene sites of the Teruel Basin for which previously only partial information was published (Godoy et al., 1983; Adrover, 1986; Mein et al., 1990).

3.4. Biochronology

Ages of sites without a first-order magnetostratigraphic calibration but positioned in a section with dated zone boundaries were constrained assuming constant sedimentation rates between boundaries. In two cases quantified evolutionary stages were used as an additional metric for age interpolation (cf. Legendre and Bachelet, 1993; van Dam, 1997; Maul et al., 1998): (*i*) quantified anagenetic (evolutionary) change in character state distributions of the *Progonomys hispanicus* – *Occitanomys sondaari* lineage was used to scale Zone K localities in the Teruel Basin (principal component scores of van Dam, 1997), and (*ii*) molar size increase in *Occitanomys adroveri* was used to scale MN12-13 sites (thereby extending on van Dam's (1997) application for the Teruel Basin). The size-ranked sequences were checked for logical inconsistencies in zone assignments ('zone test') or known superposition of beds ('superposition test').

In case no constraints could be put on the age of a locality except for its biozone, the age uncertainty range of the locality was taken maximally with regard to the biozone age uncertainty range. Locality age precision was set at 0.01 myr, which was also taken as the minimum age difference between two localities of which one was found to be 'younger' or 'older' than the other based on faunal content ('faunal stage duration convention'). Consistently, a 'faunal stage' was defined as any biochronological unit that could be distinguished from another unit by a different species/morphotype inventory. A second convention ('boundary fauna convention') was applied to rare boundary faunas, i.e., assemblages that show an overlap of taxa that normally belong to the pre- or post-boundary zone. The maximum possible duration of this overlap was set to 0.1 myr resulting in an uncertainty of ±0.1 myr for the age of a zone boundary as defined in a boundary fauna.

Karstic localities (including well-known sites such as Layna, Moreda, Belmez and Sarrión; Adrover, 1986; Castillo, 1990; Freudenthal and Martín-Suárez, 1990) were excluded from this study, as these localities tend to contain heterogeneous and potentially biased populations as evidenced by abnormally large variabilities in size and shape.

3.5. Faunal similarity and isochrony

Because of a lack of time-equivalent sets of magnetostratigraphically calibrated sections with dense fossil records (across two or more basins), the potential isochrony of local zones was evaluated indirectly. This was done by inspecting basin-to-basin similarities between (*i*) faunal assemblages, and (*ii*) species appearances and disappearances (turnover). Whereas faunal similarity helps in establishing the equivalence of local biozones across basins in order to define regional zones, similarities in turnover (i.e., shared First and Last Occurrences, FO and LO) help to understand the geological and biological contexts that underlie regional zone boundaries and their potential isochronous nature.

The rationale of looking at shared turnover is rooted in the so-called 'magnitude-frequency relationship', i.e., the observation that events with larger magnitudes occur less often than events with smaller magnitudes. The spatial corollary of this principle, which not only applies to paleontology (e.g., the 'Kill Curve'; Raup, 1991) but also to many other scientific disciplines including meteorology, seismology, and astronomy, implies that stronger events are also felt over larger areas. Thus, when the community composition in basin X changes significantly after having experienced a long period of relative stasis, the perturbing event may be assumed to be both strong and widespread. If a similar change occurs in nearby basin Y at a an approximately similar age with similar species, a single underlying event may be assumed with the two local zone boundaries necessarily being isochronous.

In our quantitative comparison of local biozones, we predominantly restricted ourselves to sites that were referred to in papers in which zonations were defined. These papers include works on the Alcoy (Mansino et al., 2017), Bajo Segura (Martín-Suárez and Freudenthal, 1998), Guadix-Baza (Piñero et al., 2018), Granada (García-Alix et al., 2008a) and Teruel Basins (Mein et al., 1990; van Dam et al., 2001; this paper). Besides the sites mentioned in these papers, we additionally used several sites from the Bajo Segura and Granada Basin that could be easily fit in biostratigraphically (Boné et al., 1978; Gamonal et al., 2018). Sites with ambiguous zone assignments (including boundary faunas) were excluded.

Faunal overlap was evaluated both qualitatively (which and how many species) and quantitatively (relative abundances). Abundances were based on the total number of first, second and third molars. In case only measured specimens were available from the literature, these were used as an alternative for total counts. 'Death assemblages', as represented by molar counts, were left uncorrected regarding differences in life expectancy (van Dam, 1997). 'Shared turnover abundance rates' (abbreviated as $STAR_A$ and $STAR_B$ for basins/areas A and B, in %) were computed as the sum of the relative abundances of disappearing and appearing species (with respect to the adjacent lower and upper zone assemblages, respectively). These were first separately calculated for each basin, and then averaged to yield one final statistic ($STAR_{A-B}$).

For the purpose of this study, two was considered the minimum number of shared species events (FO and/or LO) required in order to regard two local zone boundaries as time-equivalent, provided that the transition could not be marked as a 'rare species' event. Using Gaston's (1994) criterion for rare species as those species confined to the upper quartile of an abundance-ranked species distribution, we checked $STAR_{A-B}$ values against a value amounting to twice the average rare-common threshold percentage across all basin-zone combinations. Because most of our abundance distributions are strongly skewed towards rare species, we also checked

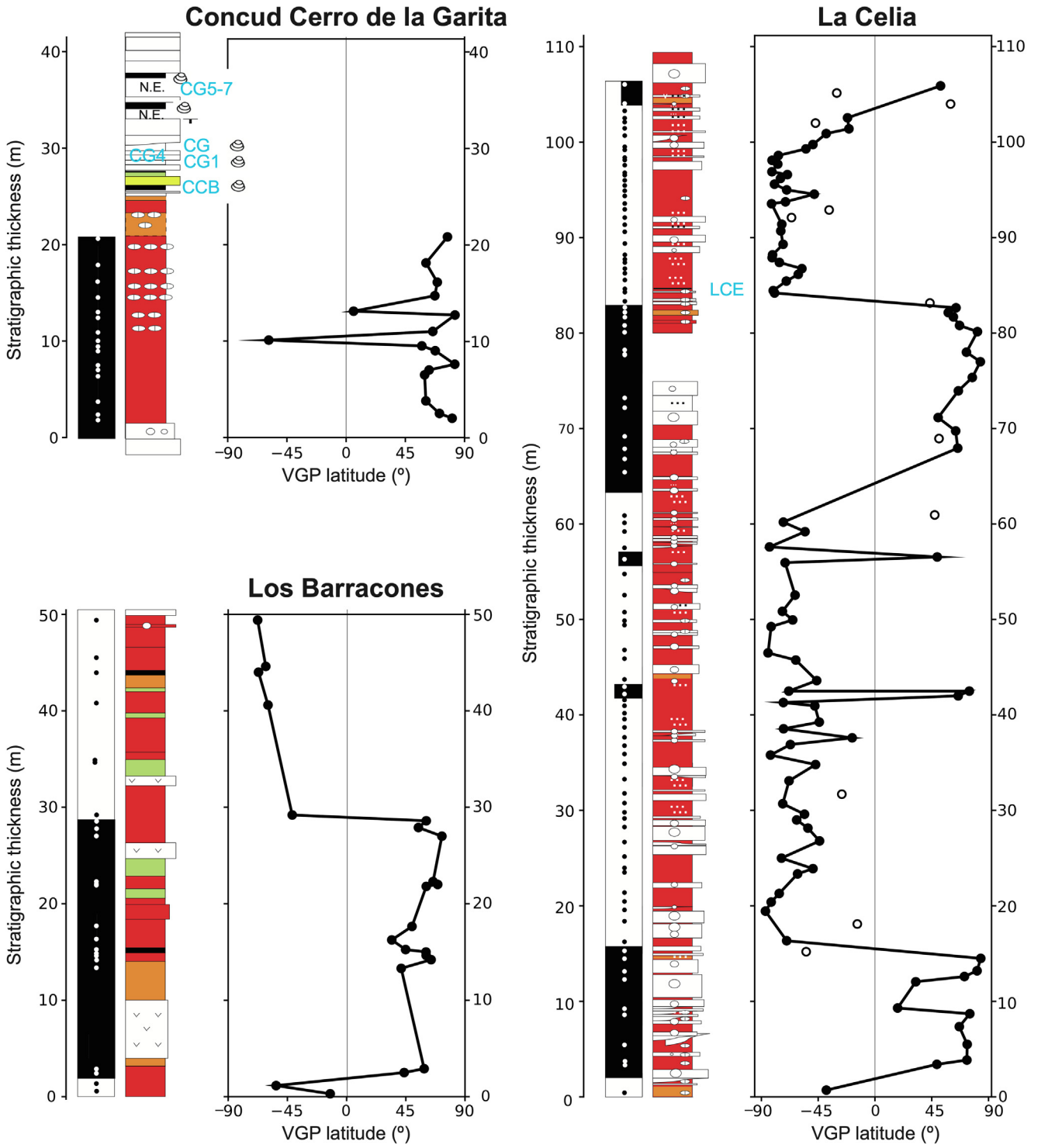

Fig. 5. Magnetostratigraphy of the La Celia (JCLC), Los Barracones (JCBA) and Concud Cerro de la Garita (CCCG) sections. Positive and negative virtual geomagnetic pole (VGP) latitudes represent normal (black) and reversed (white) polarities, respectively. For lithological symbols, see Fig. 4.

$STAR_{A-B}$ values against a threshold value based on the median of the ranked species distribution. Boundaries characterized by zero or one shared event(s) (FO or LO) or with a below-threshold $STAR_{A-B}$ value (i.e., not in the 'common regime') were thus considered suspect with regard to isochroneity. Because the records of most basins cover only a part of the studied interval, we chose to aggregate basins into three 'areas': South (S, Granada and Guadix-Baza Basin), East (E, Bajo Segura and Alcoy Basins) and Central (C, Teruel Basin). Because the records from the different basins within the areas South and East tend to alternate stratigraphically (Fig. 2), composite records for these areas could be constructed straightforwardly (i.e., mostly without between-basin averaging). Because only two zone boundaries were documented simultaneously for all three areas, we mainly focused on two-

Table 1
Mean values and Fisher statistics of paleomagnetic directions. Abbreviations: n, number of samples; Ds/Is, declination and inclination in stratigraphic coordinates; r, result of sum of unit vector; k, Fisher precision parameter; alpha95, Fisher semi angle of confidence; csd, circular standard deviation.

	Polarity	n	Ds	Is	r	k	alpha95	csd
La Celia	Normal	31	008.5	54.2	27.0	7.5	10.2	29.6
	Reversed	61	180.6	−49.6	55.2	10.4	5.9	25.2
	All samples	92	003.0	51.2	82.1	9.2	5.2	26.8
Los Barracones	Normal	15	341.3	56.8	13.6	10.3	12.5	25.3
	Reversed	7	200.6	−38.6	5.9	5.6	27.9	34.1
	All samples	22	356.2	52.9	19.0	6.9	12.8	30.9
Concud Cerro de la Garita	Normal	15	354.0	45.0	13.7	11.1	12.0	24.3
	All samples	16	356.3	46.3	14.6	10.7	11.8	24.7

area comparisons. Of the 12 boundaries that could thus be analyzed, 10 were shared between South and Central, 5 between East and Central, and 2 between East and South.

4. Results and discussion

4.1. Jumilla-La Celia Basin

Thermal demagnetization of the natural remanent magnetization (NRM) was successful in cleaning a soft viscous component at temperatures of 200–250°C in most of the La Celia and Los Barracones samples (Fig. S1, Appendix A). Above this temperature, a stable dual-polarity characteristic remanent magnetization (ChRM) was revealed. The unblocking temperature of the ChRM typically ranged between 250 and 680°C, with a marked drop of the remanence intensity at below 580°C, thus suggesting the presence of both magnetite and hematite.

According to the quality of the demagnetization data, ChRM directions were classified into three classes. Class 1 directions were calculated from linear demagnetization trajectories heading towards the origin and reaching complete demagnetization of the NRM. Class 2 directions were determined from uncomplete and scattered demagnetization trajectories heading towards the origin. Class 3 directions were defined by vector clusters denoting a stable component at 300–500°C intermediate temperatures after removal of the viscous component. The quality of paleomagnetic directions was high on average, with an average intensity of 1.2×10^{-3}A/m and an angular error <10°.

From a total of 98 samples in the JCLC section, 60 (61.2%) gave directions of class 1 and 27 samples (35.2%) of class 2. Samples of class 1 and 2 were considered to determine the magnetic polarity stratigraphy of the sections. 11 samples (11.2%) were classified as class 3 and not considered here for magnetostratigraphic purposes. With a significant set of samples of both polarities, the analysis yielded robust antiparallel normal and reversed mean directions (Fig. 5; Table 1; Fig. S2, Appendix A), indicating a demagnetization procedure that was efficient in isolating the ChRM from the secondary viscous components. From the JCBA section 7 samples (32%) gave directions of class 1 and 15 of class 2 (68%), which clearly defined a lower magnetozone of normal polarity and an upper one of reversed polarity.

4.2. Teruel Basin

4.2.1. Paleomagnetic results

The stepwise thermal demagnetization treatment of the CCCG samples yielded clear-cut results (Fig. S1, Appendix A). A viscous north-directed component representing a recent overprint was removed at low temperatures of 150–200°C. A very stable ChRM component with high unblocking temperatures up to 620°C was revealed by a linear decay trend towards the origin. According to its quality, ChRM directions of the CCCG section were grouped into class 1 (5 directions, 31%) and class 2 (11 directions, 69%), all defining a homogeneous normal polarity magnetozone (Fig. 4(F)). Only one sample in the middle of the studied interval showed an intermediate temperature (<400°C) component of reversed polarity that might represent a secondary component overprinting the ChRM signal.

4.2.2. Cyclostratigraphic and sedimentological results

The CCLP section (Fig. 4(B, C, F)) consists of 24 ± 1–2 carbonate cycles with an average thickness of 1.0 m (st. dev. = 0.18 m). Bed thickness is relatively variable in the lower part of the section (cycle 7–13) raising some doubt concerning the exact number of cycles in this interval. An uncertainty of ±1 cycle is thus assumed. A second uncertainty regarding the number of cycles is associated with a poorly exposed interval in the middle part of the section, which, given its thickness, could accommodate three cycles (18–20). Because the possibility of two thick cycles cannot be excluded, however, another +1 uncertainty in the number of cycles is assumed. Furthermore, an additional, lower set of six cycles was identified in the CCBC section (Fig. 4(E)) consisting of ∼1 m-thick, marly limestone beds of which most have indurated tops. This set, which could also be traced towards the CCCG section, was lithostratigraphically correlated to the base of the CCLP section, bringing the total number of cycles in the Concud carbonate unit to 30 ± 2.

Most carbonate beds in the CCLP section are boeuf-colored, powdery, and have a tabular/laminar structure (Fig. 4(C, D)). Based on macroscopic features, the section can be subdivided into three parts corresponding to cycles 7–13, 14–20, and 21–30. In the lower part, lignitic bands and streaks of gastropod fragments are occasionally present. In addition, the top parts of several beds contain ∼2–5 mm-thick vertical structures. The first four to five cycles of the middle part (14–20) are relatively featureless macroscopically except for the tabular/laminar bedding structure and the presence of scattered gastropod fragments. Given the same boeuf color, the poorly exposed beds on top (18–20, mentioned above) do not indicate a major change in lithology. On the other hand, cycle beds 21 and 22, which represent the transition to the upper part, are lighter (beige) colored, with bed 22 showing an indurated top part. In contrast to rock samples LP0, LP1 and LP2 from the middle part, LP3 from cycle 22 shows oxidized root remains as well as more abundant gastropods including completely preserved individuals (*Planorbarius*) (see Fig. 4(B) for the position of the samples). The upper part contains a series of beds with indurated tops (cycles 24–27) and is closed off by a brownish carbonatic marl with oriented gastropod fragments and dark pisoids (cycle 29) topped by a grey to beige indurated and recrystallized limestone (cycle 30).

The XRD analysis shows comparable mineralogical compositions of the lower five samples (LP0 to LP4, cycles 15–16 and 20–22). These samples consist of >90% calcite, with the remaining part distributed in aragonite (3–5%), gypsum (0.5–1.5%), halite (0.1–1%) and quartz (0.1–0.5%). The top samples (LP5-6, cycles 29–30) have a somewhat different mineralogical composition with less calcite

(82%) and more aragonite (13%) and quartz (2.5%) in LP5, whereas LP6 consists almost entirely of (99%) of calcite.

Microscopic inspection in plain polarized light shows that the studied rocks can be classified as biomicrites (mudstone to wackestone) with the larger components consisting of gastropod and ostracode shell material and (to a lesser degree) charophyte fragments (for representative examples, see Fig. S3, Appendix A). All thin sections except the one from LP6 show an abundant presence of black, ~20-40 μm large peloids ('clots'). Lower samples LP0, LP1 and LP2 are clearly laminated, with irregular ~100–200 μm thick lamina consisting of an alternation of reddish micritic layers and whitish cemented layers ('laminated micrites' *sensu* Freytet and Verrecchia, 2002). The whitish layers contain strongly fragmented biogenic carbonate, although locally recognizable charophyte fragments (stems, gyrogonids and encrustations) can be seen. Whereas clot accumulations follow the laminar structure in LP0, clots are more homogeneously distributed in the higher samples. A decrease in lamination from LP0 and LP4 is accompanied by an increase in the frequency of thin cracks filled with micrite/microsparite, and with the preservation of complete shells. LP5 shows a further increase in the abundance and thickness of cracks and in the abundance of shell material (especially of well-preserved ostracode shells). The thin section of top sample LP6 (cycle 30), on the other hand, shows a massive, recristallyzed micrite without clearly recognizable fossils.

The combined macroscopic, microscopic and mineralogical evidence points to the evolution of a low-energy, shallow lake system with deepest lake levels corresponding to middle part of the LP section (cycles 14–20, 'shallow permanent lake facies'; Abels et al., 2009a). Whereas indications for subaerial exposure, plant reworking and nearness to the lake shore are generally lacking in the middle part, evidence for such conditions are present in the lower and especially upper part of the section ('very shallow transient lake facies'; Abels et al., 2009a). However, except for the top part, carbonate reworking in the LP section appears less intense than in other time-equivalent parts of the basin (e.g., palustrine limestones facies in Alonso-Zarza and Calvo, 2000).

Because orbitally (precession)-controlled groundwater fluctuations have been shown to underlie shallow lacustrine / mudflat oscillations in the Teruel Basin (MN9-10; Abels et al., 2009b), and because a similar mechanism was hypothesized concerning the origin of sedimentary cycles in our study interval (MN11/12; Alonso-Zarza et al., 2012), we feel confident in interpreting the sedimentary cyclicity in the CCLP section as the result of precession-controlled changes in humidity and lake level. (Obliquity can be confidently ruled out as the dominant orbital component, as upward counting of 41-kyr cycles would lead to an age of ~6.7 Ma for CC3, implying a MN13 instead of MN12 age.)

4.2.3. Paleontological results

All rodent species found at Concud were previously described by van de Weerd (1976) with the following exceptions (see Suppl. Text, Appendix A): (*i*) four small-sized, primitive-looking molars from CCCG were designated as Murinae indet., and (*ii*) two specimens from CG7 resembling *P. barbarae*, were named *Parapodemus* aff. *barbarae*, because of their relatively large width compared to *P. barbarae*. Possibly these specimens represent the evolutionary transition towards *P. meini* (Martín-Suárez and Freudenthal, 1993).

R5A and R5B yielded poorly diversified micromammal faunas that are somewhat atypical. *Occitanomys adroveri* is abundantly present in both levels, whereas murines normally associated with this species in the basin in Zone L such as *Parapodemus barbarae* and *Huerzelerimys turoliensis* are lacking (three very worn specimens in R5B may however represent the latter form; see Suppl. Text, Appendix A).

Instead of *Parapodemus barbarae*, R5A contains two small-sized molars identified as *P. lugdunensis*, a form otherwise known from lower Zone K. Similar small-sized specimens previously assigned to *P. barbarae* occur in Valdecebro 5 (VDC5; Adrover et al., 1986: their Fig. 4(B, C, E)), a locality also lacking *H. turoliensis*. These specimens are here re-assigned to *P. lugdunensis*. Finally, our re-inspection of the murine material from basal M1 site Masada del Valle 6 (MDV6, van de Weerd, 1976) revealed a small-sized and slender M2, which was previously assigned to *P. barbarae*, but which we consider belonging to the same species (*P.* cf. *lugdunensis*). Hence, the re-appearance of *P. lugdunensis* in the basin is thus confined to a short interval consisting of the upper part of Zone L and basal part of Zone M1.

In order to accommodate the deviating faunas of R5A and VDC5 biostratigraphically, we define a new local zone, the *Parapodemus barbarae* – *Castromys inflatus* Interval-Zone, which is coded by L2 (Fig. 2). The previously defined *Parapodemus barbarae* Interval Zone (Zone L, van Dam et al., 2001), of which until now the top was defined by the entry of *Stephanomys ramblensis* (van de Weerd, 1976) is redefined as the *P. barbarae* Range Zone (L1). Whereas L1 thus contains *P. barbarae* and *Huerzelerimys turoliensis,* L2 lacks both these species but contains *P. lugdunensis*. In addition, L2 differs from L1 by the larger size of *Occitanomys adroveri*.

The present work seems the appropriate place to rename the local Pliocene zones of Mein et al. (1990) in line with the international stratigraphic guidelines (Interval Zones; Salvador, 1994; Fig. 2). We additionally apply the lettered codes N1-O4 to these zones, thereby extending on the Miocene codes J1-M3 of van Dam et al. (2001) and the N1, N2 and O codes of Morales et al. (2013). We (as in Mein et al., 1990) slightly depart from Morales et al.'s definitions in not using the entry of *Promimomys* as a local stratigraphic criterion. Although *Promimomys* has a wide distribution and its FO is used as a marker for European unit MN14 (Hilgen et al., 2012), it is very rare on the Iberian Peninsula, rendering the event less useful for Iberian biostratigraphy. With sole occurrences in Teruel Basin localities La Gloria 4, Celadas 9 and 12, the entry of *Promimomys* in Spain can be shown to post-date that in southeastern Europe, where it is dated between 5.40 and 5.23 Ma (Hordijk and de Bruijn, 2009; see Section 4.3.2 for discussion). For this reason, we basically retain Mein et al.'s (1990) 'Zone à 2 *Paraethomys*' (renamed here as *Paraethomys baeticus* – *Trilophomys* interval Zone) and accompany it by the code N2, which now encompasses both Morales et al.'s Zone N2 (without *Promimomys*) and the lower part of their Zone 'O' (with *Promimomys*). N3 is used for Mein et al.'s (1990) '*Trilophomys* Zone'. Finally, we introduce the new letters O1-4 to cover Mein et al.'s (1990) four youngest zones (approximately corresponding to MN16 and MN17), thereby avoiding alphabetic overlap with the previously defined Oligocene Zones P, Q, etc. in the Spanish interior region (Álvarez Sierra et al., 1987).

The revisions of Cricetinae by Freudenthal et al. (1991, 1998) urged a re-inspection of the Teruel Basin material of this group. We concluded that the identifications of *Neocricetodon occidentalis* and *Apocricetus alberti* in van Dam et al. (2001) can be retained, but that the Ib-N12 and N13a populations previously identified as *N.* ('*Kowalskia*') *occidentalis* should be transferred to *Apocricetus* aff. *plinii*. Furthermore, the cricetines from Valdecebro 6, Arquillo 1 and Villastar, which, according to Adrover et al. (1993) belong to the same species as the one from La Gloria 5, are considered to represent *A. alberti* (for details, see Suppl. Text, Appendix A).

All faunal lists and specimen measurements are included in Tables S1 and S2 (Appendix A).

4.3. Iberian rodent biozones

4.3.1. Justification

As can be seen in Fig. 6(A), all abundance-based basin-to-basin similarities between assemblages for time-equivalent biozones

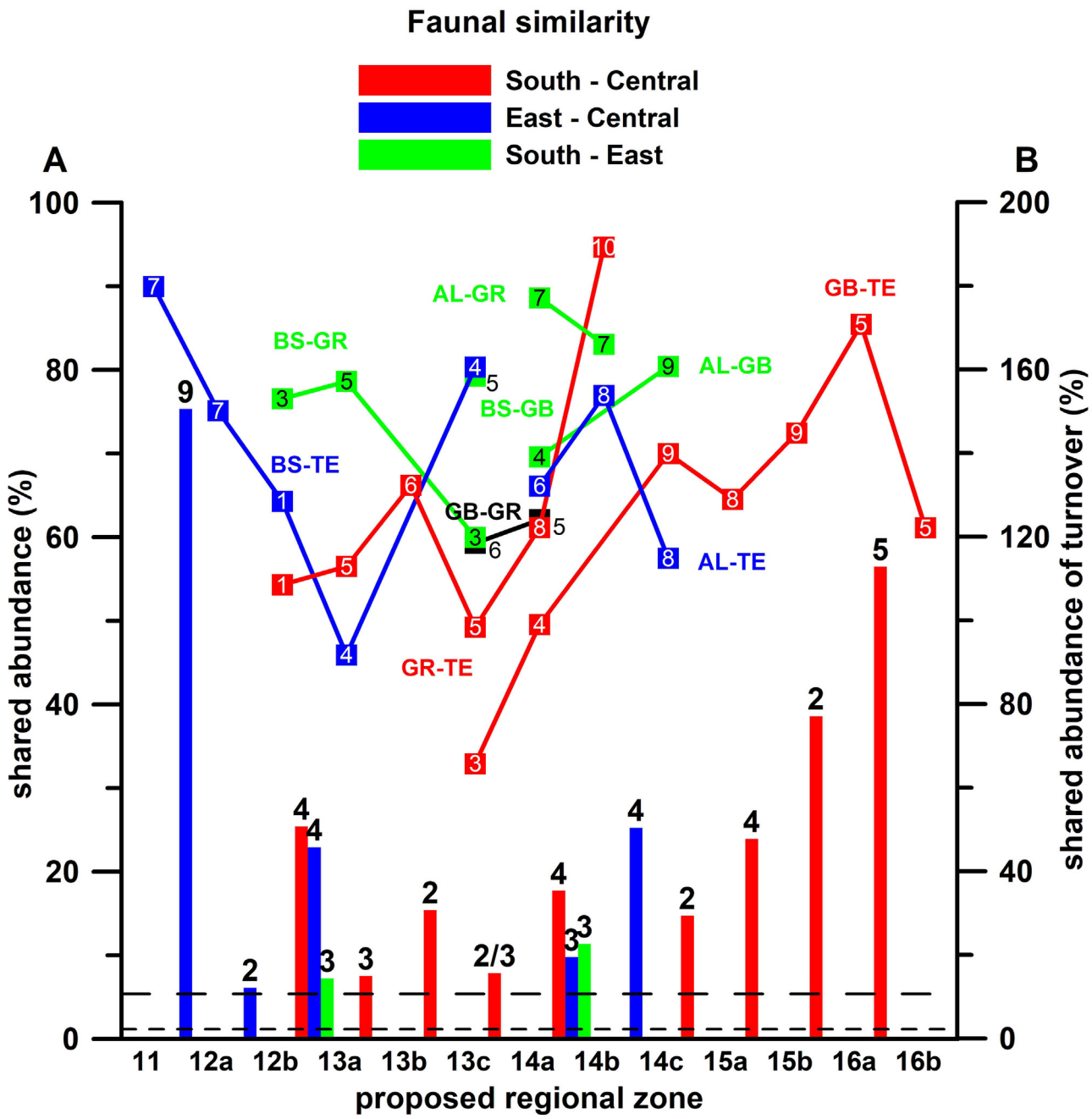

Fig. 6. Similarities between rodent assemblages and turnover for individual basins for the proposed system of Iberian zones (see section 4.3.2 for formal definitions, and Tables S1, S3, Appendix A, for selected localities and data, respectively). **A**. Lines and squares: relative abundance of shared species (averages for basin pairs); numbers in squares: numbers of shared species. Abbreviations: AL, Alcoy Basin; BS, Bajo Segura Basin; GB, Guadix-Baza Basin; GR, Granada Basin; TE, Teruel Basin. **B**. Bars: rates of shared turnover (FO + LO) between East, South, and Central areas (Fig. 1); numbers above bars: numbers of shared species events; dashed lines: average rare-common threshold level based on quartile (lower line) and median (upper line) of ranked abundance distribution (see Section 3.5).

except one have values in the range 50–95%. The overall high levels of similarity, which correspond to an average number of six overlapping species, underline the validity of the correlation scheme as shown in Fig. 2. High numbers of seven to nine or ten shared species characterize the oldest Late Miocene intervals ('11' and '12a') and a large part of the Pliocene (Ruscinian, '14a' to '15b'). Numbers drop to five in the early Villanyian ('16a' and '16b') as recorded for the Guadix-Baza – Teruel Basin pair. The low similarity between these two basins for level '13c' (Fig. 6(A)) partly depends on the use of different chronospecies (in *Apodemus* and *Stephanomys*), which, in turn, may be the result of the considerable time span covered by this zone (see below) in combination with a low locality density. On the other hand, the high abundance-based similarity between the Bajo Segura and Teruel Basin for level '12b' is caused by the contribution of one dominant species only (*Occitanomys adroveri*).

Shared turnover results are shown in Fig. 6(B) (for underlying data, see Table S3, Appendix A). First, average threshold values of 1.1% and 2.7% were computed for separating rare from common species using the quartile criterion (Gaston, 1994) and median criterion, respectively. In combination with our required minimum of two appearing/disappearing species, we thus consider boundaries

Table 2
Chronology of Iberian rodent zone boundaries. Ages are calibrated to the time scale of Raffi et al. (2012). Uncertainty ranges are based on ages of bracketing or transitional localities indicated.

Rodent Zone boundary	Lower Zone	Upper Zone	Lower bracketing site*	Upper bracketing site*	Transitional site	Max. age (Ma)	Min. age (Ma)	Uncertainty (myr)
top Ib-N17b	*Mimomys realensis*		Valdeganga IV	FA *Allophaiomys pliocaenicus*		1.90	1.80	0.10
Ib-N17a-b	*Mimomys medasensis*	*Mimomys realensis*	Villarroyo	Fuentenueva, Alquería	Valdeganga II (Cortez de Baza 1,6)	2.15	2.05	0.10
Ib-N16b-17a	*Kislangia ischus*	*Mimomys medasensis*	Concud Estación 2	Valdeganga I		2.56	2.54	0.02
Ib-N16a-b	*Mimomys hassiacus*	*Kislangia ischus*	Gea 0	Zújar 11		3.06	3.03	0.03
Ib-N15b-16a	*Dolomys adroveri*	*Mimomys hassiacus*	Escorihuela B	Zújar 10	Escorihuela C	3.19	3.18	0.01
Ib-N15a-b	*Mimomys davakosi*	*Dolomys adroveri*	Villalba Alta 4	Villalba Alta 2		4.01	3.92	0.09
Ib-N14c-15a	*Trilophomys castroi*	*Mimomys davakosi*	Villalba Alta Rio 1	Zújar 4		4.27	4.19	0.08
Ib-N14b-c	*Paraethomys baeticus*	*Trilophomys castroi*			Sifón de Librilla P	4.71	4.51	0.20
Ib-N14a-b	*Apocricetus barrierei*	*Paraethomys baeticus*	Fuente del Viso	La Bullana 3	(Peralejos E)	4.91	4.87	0.04
Ib-N13c-14a	*Paraethomys meini*	*Apocricetus barrierei*	Zorreras	Sifón de Librilla 413 (La Alberca)		5.47	5.33	0.14
Ib-N13b-c	*Apocricetus alberti*	*Paraethomys meini*	Sifón de Librilla 52	Venta del Moro		6.26	6.25	0.01
Ib-N13a-b	*Castromys inflatus*	*Apocricetus alberti*			El Búnker 4/5	6.56	6.27	0.29
Ib-N12b-13a	*Parapodemus meini*	*Castromys inflatus*	El Búnker, *Crevillente 17*	El Chorrico 17 (Masada del Valle 6)		7.02	6.90	0.12
Ib-N12a-b	*Huerzelerimys turoliensis*	*Parapodemus meini*	*Los Aljezares 2B*	La Celia		7.18	7.09	0.09
Ib-N11-12a	*Huerzelerimys vireti*	*Huerzelerimys turoliensis*	Balneario	Fuente Podrida, Concud B/L	(Crevillente 4)	7.68	7.65	0.03
base Ib-N11		*Huerzelerimys vireti*	La Gloria 11	Los Aguanaces 7		8.75	8.63	0.12

* Sites in regular print: magneto/cyclostratigraphic constraint; sites in italic print: sedimentary or evolutionary rate constraint; sites in brackets: derived constraint (see text).

with $STAR_{S-C}$, $STAR_{E-C}$, or $STAR_{E-S}$ values exceeding 2.2-5.4% as basically isochronous.

A very high $STAR_{E-C}$ value of 150% involving no less than nine species leaves little doubt for isochrony of the oldest local zone boundaries, i.e., the ones between the *Huerzelerimys vireti* and *Parapodemus barbarae* Zones in the Teruel Basin and between the *Occitanomys sondaari* and *H. turoliensis* Zones in the Bajo Segura Basin (Fig. 6(B)). According to the magnitude-frequency relationship, we are dealing with a strong event affecting a large area. The same reasoning applies to the uppermost boundary between zones with *Mimomys hassiacus* and zones with *Kislangia ischus*, which involves five species events and for which a $STAR_{S-C}$ value of 113% is computed. (Note that the *M. hassiacus* and *M. polonicus* Zones in the Guadix-Baza Basin are combined, see Section 2.1).

Although all boundaries satisfy our combined criteria of a minimum of two species and a STAR value >2.2 or even 5.4% (Fig. 6(B)), several transitions deserve some additional discussion given their relatively low values (<20%):

- During the '12a'–'12b' transition, *H. turoliensis* and *Eliomys* sp. A disappear with an associated $STAR_{E-C}$ value of 12%. On the other hand, both areas (East and Central) undergo a major change in their fauna: seven additional species (with abundance >0.1%) disappear in the central part (Teruel Basin) and eight (different) species experience their FO or LO in the eastern Bajo Segura Basin (Table S3, Appendix A). In this particular case, we consider it a probable scenario that one single event of considerable magnitude resulted in extinction in one area and replacement in another. The fact that faunas in East and Central became very different during '12b' (Central has only one species in common with East and South, Fig. 6(A)) points to a strong difference in environmental conditions and/or the temporary presence of a barrier. Sampling (a poor representation of localities, e.g., two sites in the Teruel Basin) may play an additional role;
- The low $STAR_{E-S}$ value compared to much higher $STAR_{S-C}$ and $STAR_{E-C}$ values at the '12b'–'13a' transition is due to the exceptional dominance of *Occitanomys adroveri* (e.g., 72% in the Granada Basin) affecting the relative abundances of characteristic taxa entering together such as *O. alcalai*, *Castromys inflatus* and *Stephanomys*. Despite the low STAR value, we regard the common entry of these three species and the overall magnitude of faunal change during the transition (Fig. 6(B)) as a positive indication for a single underlying event affecting all three faunas approximately coevally;
- Three shared species and a $STAR_{S-C}$ value of 14.9% characterize the '13a'–'13b' transition. It should be noted that the strong expansion of *Apodemus* is not represented as an event in the calculation. Present with very low numbers in both lower zones (as *A.* sp. indet. and *A. gudrunae*, respectively), this genus turns into one of the dominant forms in both upper zones (as *A.* aff. *gorafensis*/*A. gorafensis*, and *A. gudrunae* in South and Central, respectively) with percentages of 50% and 31%. If this expansion of the *A. gudrunae* – *A. gorafensis* lineage would be counted as a boundary 'event', shared abundance would be considerably higher. On the other hand, *A. gudrunae* is already common (19%) in basal '13a' site SIF1 in the Fortuna Basin (Piñero and Agustí, 2019), which is not included in the similarity calculations because no local zonation has yet been defined for this basin;
- Shared species events at the '13c'–'14a' transition include the LO of *Apocricetus alberti* and the FO of *A. barrierei*. The Granada Basin additionally shares the entry of *Celadensia nicolae* with the

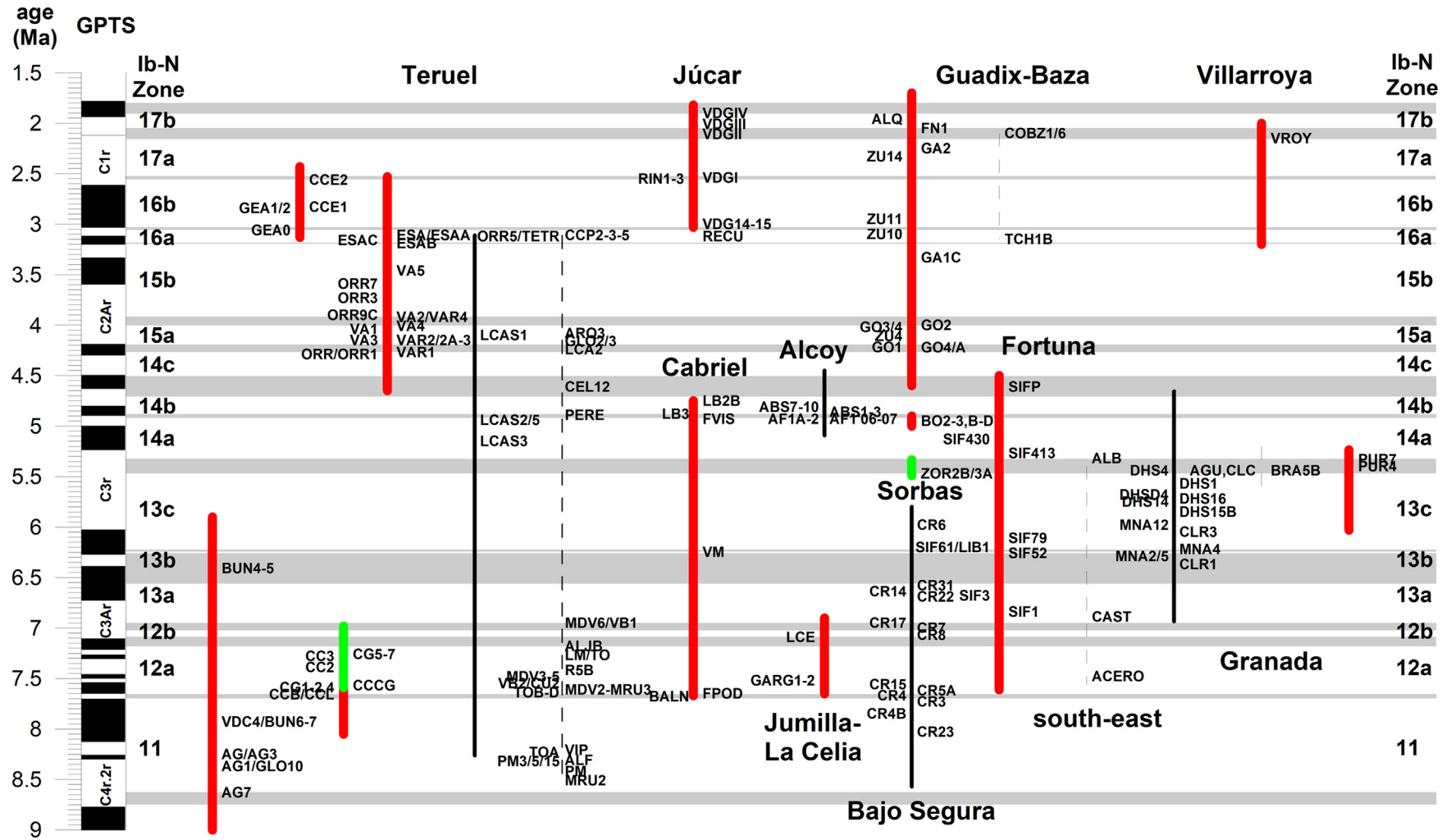

Fig. 7. Chronological placement of Iberian micromammal localities with age uncertainty ≤200kyr. Shown are magnetostratigraphically calibrated sections (thick red lines), cyclostratigraphically calibrated sections (thick green lines), sections for which constant sedimentation rates are assumed (thin black lines), intervals with locality ages estimated otherwise (dashed lines), and Ib-N Zone age uncertainty ranges (grey bars). Ages are calibrated to the time scale of Raffi et al., 2020. For full locality names, see Table S1 (Appendix A).

Teruel Basin. Whereas this form represents the most abundant rodent in the latter basin, it is very rare in the former, however. STAR values for the Granada-Teruel and Guadix-Baza-Teruel comparisons are 26.1% and 5.1%, respectively, with their average value shown in Fig. 6(B). (Pooling the raw data for both southern basins would have been another option; in this case the resulting STAR value would have been approximately equal to the highest value.) We finally note that *Apocricetus* is rare in the Teruel Basin and that not all cricetine molars found in localities Celadas 3 and 4B could be assigned with certainty to *A. barrierei* (as positively identified in Celadas 4B; see Table S3, Appendix A).

Overlooking all the evidence on faunal similarity and shared turnover, we consider the transfer of Iberian zone boundary ages across basins a viable step in the process of locality age estimation for our entire study period.

4.3.2. Iberian rodent zones

The new regional zonation presented here (Table 2; Fig. 7) will also include MN17-correlative biozones, even though these were defined in one basin only (Guadix-Baza Basin) and could therefore not be subjected to faunal similarity analysis. The possibility of applying these zones to a wider area is nevertheless suggested by observations in the Júcar Basin (Valdeganga section, eastern Spain), where the two name-giving species for the Guadix-Baza zones (*Mimomys medasensis* and *M.* cf. *reidi*) appear in the same order (Mein et al., 1978; Opdyke et al., 1997).

Iberian zones are applied to all studied areas within the Peninsula except for the La Cerdanya Basin (Pyrenees). The MN13-correlative fauna Can Vilella from this basin has an atypical, more central European-type of rodent fauna that lacks typical Iberian murines (Agustí et al., 2006b). The only murine reported is *Apodemus gudrunae*, known from MN13-correlative sites on the Peninsula. The second form with a distinct Iberian record is the insectivoran *Amblycoptus jessiae* (Furió and Agustí, 2017). This soricid enters the Teruel Basin record around the M1-2 transition and becomes especially abundant in Zone M2 (also MN13, e.g., Las Casiones; van Dam, 2004). In our view, the Iberian Zone system cannot be applied to Can Vilella, which should be placed in another regional (French/Central European) system.

Opting for assemblage zones and following the international stratigraphic rules (Salvador, 1994), we name the new zones after the (or one of the) most commonly occurring species (Table 2). In order to preserve the aspect of chronological ranking, a parallel system of codes was set up. These codes start with 'Ib-N' (Iberian Neogene) and are followed by a number (11, 12, etc.) that roughly corresponds to the time-equivalent MN unit, and a letter to indicate the actual Zone (Ib-N12a, Ib-N12b, etc.). For consistency reasons, we retain the number 17 as in MN17, although this unit now formally belongs to the Quaternary (Gradstein et al., 2012). The use of MN unit numbers is only meant for convenience (i.e., rapid chronological appreciation) and has no significance in terms of strict correlation. We will now name and describe all biozones, mention the most important qualitative and quantitative differences between basins, and provide age uncertainty intervals for zone boundaries (Table 2). For the sake of brevity, we use shortened forms of the zone codes in the main text body, i.e., omitting the prefix 'Ib-'.

The ***Huerzelerimys vireti* Zone** (**Ib-N11**, early Turolian, late Tortonian) is quantitatively dominated by small-sized murines. Whereas *Occitanomys sondaari* is dominant in the Teruel Basin, *Parapodemus lugdunensis* and the cricetine *Neocricetodon* are more important in the Bajo Segura Basin. The jumping mouse *Eozapus* shows a modest but persistent presence in the Teruel Basin but is absent in the Bajo Segura Basin.

The base of N11 is dated in the Teruel Basin to lie between 8.75 (La Gloria 11) and 8.63 Ma (Los Aguanaces 7) based on magnetostratigraphic results for the La Gloria – El Búnker sections (Krijgsman et al., 1996; van Dam et al., 2001).

In the ***Huerzelerimys turoliensis* Zone** (**Ib-N12a**, middle Turolian, late Tortonian), *Parapodemus lugdunensis* is replaced by the larger-sized *P. barbarae*. *Occitanomys* (*O. adroveri*) loses its dominance within murines. Within the cricetines, *Neocricetodon* is replaced by *Apocricetus* aff. *plinii* in the Teruel Basin, and by *Cricetulodon meini-lucentensis* lineage in the Bajo Segura and Fortuna Basins.

The N11-N12a boundary is dated in the Cabriel Basin at 7.68–7.65 Ma based on the magnetostratigraphy and sedimentation rate of the Cabriel North section (Opdyke et al., 1989, 1997), with locality Fuente Podrida placed at the base of C4n.1n (Table S4, Appendix A).

The ***Parapodemus meini* Zone** (**Ib-N12b**, middle Turolian, early Messinian) is characterized by the absence of *Huerzelerimys*. Of all zones, inter-basinal differences are the largest. Whereas *Occitanomys* (*O. adroveri*) becomes even more dominant in the Teruel Basin and the *Parapodemus barbarae-Castromys* lineage disappears, the latter lineage becomes well represented in the Bajo Segura and especially in the Granada Basin.

The N12a-12b boundary is estimated to lie between 7.18 and 7.09 Ma. The lower limit corresponds to the maximum age of N12a site Aljezar 2B (ALJB) in the Teruel Basin, as inferred from extrapolating evolutionary rates (M1 size) of *Occitanomys adroveri* (see Section 4.4.4) calibrated to cyclostratigraphically inferred locality ages in the Concud sections (see Section 4.4.1). The upper limit (7.09 Ma) corresponds to the age of N12b site La Celia (Jumilla-La Celia Basin; Section 4.4.1, options II/III). The marine Tortonian-Messinian boundary (7.25 Ma) correlates to the upper part of N12a.

Assemblages belonging to the ***Castromys inflatus* Zone** (**Ib-N13a**, late Turolian, early Messinian) strongly differ from those in the previous Zone. *Stephanomys* is now well represented in central Spain (Teruel and Madrid Basins) where it has replaced *Occitanomys adroveri*, while this latter form remains dominant in the South (Granada Basin). Presence of *Stephanomys* and absence of *Occitanomys adroveri* also characterizes the East (Fortuna Basin). At the same time, the locus of maximum abundance of *Castromys* moves northward (Teruel Basin).

A lower limit of 6.88 Ma for the N12b-13a boundary follows from the age of 6.87 Ma for N13a site El Chorrico 17 in the Fortuna Basin (Garcés et al., 1998) and the reservation of an additional (minimum) duration of 0.01 myr for basal N13a site Masada del Valle 6 (Teruel Basin). Although an explicit faunal list for El Chorrico 17 has not yet been published, the locality is part of a set of sites (Agustí et al., 2006a: table 1) that is characterized by the presence of an advanced *Castromys* species, and of *Apodemus gudrunae* and *Apocricetus alberti*, forms that imply a faunal stage younger than Masada del Valle 6. This latter locality is considered to represent a separate 'faunal stage' (see Section 3.4) between the 'regular' N12b and N13a faunal stages based on the absence of *Occitanomys alcalai*, the presence of *Parapodemus* cf. *lugdunensis* (see Suppl. Text, Appendix A) and the insectivoran *Archaeodesmana luteyni* (Rümke, 1985). Based on the assumption of a constant sedimentation rate in the Crevillente section (Bajo Segura Basin), the maximum age of the boundary can be constrained to 7.02 Ma (maximum age for Crevillente 17, see Section 4.4.3).

With *Castromys* disappearing and *Occitanomys adroveri* rarifying, other murine taxa such as *Occitanomys alcalai* and *Apodemus gudrunae* increase their relative abundance in the ***Apocricetus alberti* Zone** (**Ib-N13b**, late Turolian, middle Messinian). The cricetine *Apocricetus* (re-)appears in the various basins as the name-giving *A. alberti*. Although in small numbers, the entry of the cricetodontine *Blancomys* is noteworthy.

The N13a-b boundary cannot be estimated very accurately. The magnetostratigraphically constrained site El Búnker 4/5 (Teruel Basin) is a 'boundary locality' (see Section 3.4), given the combined presence of *Castromys inflatus* and the insectivoran immigrant *Amblycoptus jessiae*. The fauna, with an age estimate between 6.46 and 6.37 Ma (Table S4, Appendix A), can be placed between typical N13a faunas with *Castromys inflatus* (El Búnker, La Gloria 6) and N13b faunas (Las Casiones, Las Casiones Superior, Las Casiones Superior A, Villastar, Valdecebro 6, La Gloria 5) without this species but with *Apocricetus alberti*, *Blancomys sanzi* and *Amblycoptus jessiae* (van Dam, 2004). Applying the 'boundary fauna convention' (see Section 3.4), the age of N13a-b boundary is constrained to 6.56–6.27 Ma. The younger limit is a very conservative estimate, because placing boundary at 6.27 Ma would leave almost no space to accommodate N14b localities, given the age of the N13b-c boundary (see below).

The composition of the ***Paraethomys meini* Zone** (**Ib-N13c**, late Turolian, late Messinian) is like that of the previous zone, except for the addition of the African immigrant *Paraethomys meini*. Whereas a low percentage of ~5% of this species characterizes the Teruel Basin, larger shares of 20–30% characterize the southern and eastern basins.

The entry of *Paraethomys* defining the N13b-c boundary is magnetostratigraphically constrained in the El Chorrico and Sifón de Librilla sections in the Fortuna basin (Garcés et al., 1998; Agustí et al., 2006a; Piñero and Agustí, 2019). Assuming constant sedimentation rates within polarity zones and ignoring sample size effects, the base of N13c can be dated to lie between ~ 6.26 Ma (SIF52) and 6.20 Ma (SIF61 = Librilla; Gibert et al., 2013) in the Sifón de Librilla section, or between 6.15 Ma (AU2-r) and 6.03 Ma (AU3-a) in the El Chorrico section. However, because *Paraethomys* is already present in the 6.25 Ma old locality Venta del Moro in the Cabriel Basin (Gibert et al., 2013), we use 6.26–6.25 Ma as the boundary age between N13b and c, while regarding the absence of *Paraethomys* in the AU2 levels as a sampling effect.

The composition of the ***Apocricetus barrierei* Zone** (**Ib-N14a**, Turolian-Ruscinian transition, Messinian-Zanclean transition) is not very different from that of the *Paraethomys meini* Zone, except in the North (Teruel Basin), where the 'microtoid cricetid' immigrant *Celadensia nicolae* constitutes 45% of the rodent fauna. The murine *Occitanomys brailloni* is for the first time present in the East and South (Fortuna Basin, Guadix—Baza Basin, Caravaca), whereas hamsters (*Ruscinomys*, *Blancomys*, *Apocricetus*) increase their share in the South (Purcal 4, Granada Basin). The large percentage of *Paraethomys meini* in the Alcoy Basin (55%) is remarkable.

The lower age limit of the N13c-14a boundary is represented by the localities Zorreras 2B and 3A in the Sorbas Basin, which are magnetostratigraphically constrained to C3r (Martín-Suárez et al., 2000). With the immigrant *Debruijnimys almenarensis* and relatively small-sized murines present, the Zorreras localities can be confidently assigned to Zone N13c. Their age can be narrowed down to 5.47 Ma by acknowledging their stratigraphic position within the 'Zorreras Member', a sediment package of 8 precession cycles that is time-equivalent to the latest Messinian Lago Mare phase (Krijgsman et al., 2001) and which ends with the Pliocene flooding event at 5.33 Ma. Ages well over 5 Ma for the upper age limit can be inferred based on magnetostratigraphy at Sifón de Librilla 413 and 430 (Fortuna Basin; Agustí et al., 2006a; Piñero and Agustí, 2019). Although the presence of *Debruijnimys julii* (known from N14b site La Bullana 2B and N14c site Baza) could suggest a higher zone, the inclusion of SIF413 into Zone N14a is not only supported by its numerical age (5.27 Ma; Garcés et al., 1998; Agustí et al., 2006a; Piñero and Agustí, 2019), which would exclude N14b and c, but also by the absence of a large-sized *Paraethomys* lineage, of which the entry corresponds to the base of Zone N14b. With sites Sifón de Librilla 413 and 430 (5.13 Ma and 5.27 Ma, respectively) belonging to N14a, the N13c-14a boundary can be assumed to be older than 5.27 Ma. On the other hand, a boundary older than the Mio-Pliocene boundary (5.33 Ma) can be inferred from the classical fauna of La Alberca, a site interbedding with marine Messinian sediments that can be assigned to N14a (presence of *Apocricetus barrierei*). Here we conservatively set the minimum age of the N13c-14a boundary to 5.33 Ma.

The proximity of the younger limit of the N13c-N14a boundary to the Miocene-Pliocene boundary and marine Messinian-Zanclean boundary (5.33 Ma) leaves the possibility open that both boundaries are (almost) coeval. The approximate correlation of N13c-N14a boundary to the transition from European Mammal unit MN13 to MN14 as implied by our zone numbering system thus also entails an approximate correlation of this MN transition to the Miocene-Pliocene boundary (5.33 Ma). However, it should be noted that such a correlation is based on the 'faunistic interpretation' of the MN system. If the 'stratigraphic interpretation' of the MN system would be adopted (see Hilgen et al. (2012) for these two interpretations), the key defining event would be the First Historical Appearance of *Promimomys* in Europe, which is dated to 5.40–5.23 Ma in Greece (see Section 4.2.3). Although this age range is comfortably close to that of the Ib-N13c-14a boundary, it has also become clear that direct use of the *Promimomys* entry in Spain may lead to erroneous age correlations, because of its potential diachroneity as evidenced by some rare occurrences in Zone N14b only. In this respect, the First Historical Appearance of *Occitanomys brailloni* could be a better candidate to mark the transition from MN13 to MN14 (Piñero and Verzi, 2020), especially because this species is also recorded for the first time in MN14 faunas in the eastern Mediterranean region (Koufos and Vasileiadou, 2015) with a dated first occurrence between 5.20 Ma and 5.04 Ma (Hordijk and de Bruijn, 2009). On the other hand, *O. brailloni* is absent from many N14a-b-c sites on the Iberian Peninsula where it starts to become a common resident only from N15a onwards (Table S1, Appendix A).

After the rapid disappearance of *Celadensia*, compositions become more homogeneous across the Iberian Basins in the ***Paraethomys baeticus* Zone** (**Ib-N14b**, early Ruscinian, early Zanclian). *Paraethomys baeticus*, *P. meini* and *Occitanomys alcalai* are the most important species. *Apocricetus* is the most abundant lineage in the Cabriel Basin.

The N14a-b boundary is constrained to 4.91–4.87 Ma. The maximum age of 4.91 Ma is based on the age of 4.93 Ma of N14a locality Fuente del Viso (Cabriel Basin; Opdyke et al., 1997) lowered by an additional 0.01 myr in order to accommodate the N14a-b boundary fauna Peralejos E (Teruel Basin). Similarly, the minimum age of 4.87 Ma is constrained by the assumed minimum age of 4.85 Ma for the N14b site La Bullana 3 (Cabriel Basin), which is correlated to C3n.3n (see Section 4.4.3 and Suppl. Text, Appendix A).

The transition to the ***Trilophomys castroi* Zone** (**Ib-N14c**, early Ruscinian, early Zanclean) is characterized by a second immigration of 'microtoid cricetids' as represented by *Trilophomys*, a form of unknown cricetine origin not directly related to *Celadensia* (Fejfar et al., 2011). In its way of expansion, *Trilophomys* mimics *Celadensia* in becoming immediately, although temporary, dominant in central Spain (~50% in the Teruel Basin), while forming only a modest addition to the existing fauna in the South (~5% presence in the Alcoy and Guadix-Baza Basins; the latter basin witnesses a distinct expansion of *Apocricetus* instead).

With *Stephanomys cordii* present, but *Trilophomys* still absent, Sifón de Librilla P (Fortuna Basin) can be regarded as a 'boundary fauna' between Zones N14b and 14c. We therefore take its magnetostratigraphically dated age of 4.61 Ma as an estimate for the central age of the N14b-c boundary, while adding ±0.1 myr (4.71–4.51 Ma, see convention in Section 3.4).

In the ***Mimomys davakosi* Zone** (**Ib-N15a**, middle Ruscinian, middle Zanclean) *Trilophomys* is largely replaced by the arvicoline *Mimomys davakosi*. Instead of *M. davakosi* and *Trilophomys*, the eastern fauna of La Juliana is still dominated by *Paraethomys* (two lineages).

The age of the N14c-15a boundary is constrained to lie between 4.27 Ma and 4.19 Ma, based on magnetostratigraphic calibrations in the Villalba Alta Río section (Teruel Basin; Opdyke et al., 1997) and Zújar section (Guadix-Baza Basin; Oms et al., 1999) with ages of 4.27 Ma for Villalba Alta Río 1 (N14c) and 4.19 Ma for Zújar 4 (N15a, with *Mimomys* cf. *davakosi*).

The large-sized arvicoline *Dolomys adroveri* replaces *Mimomys davakosi* in the ***Dolomys adroveri* Zone** (**Ib-N15b**; late Ruscinian, late Zanclean). It occupies an important share of the rodent fauna in both the central (Teruel Basin) and southern (Guadix-Baza Basin) parts of the Peninsula. Relatively heterogeneous Ib-N14c-15a faunas with *Paraethomys* and *Apocricetus* are replaced by a poorly diversified fauna in the latter basin that, besides by *Dolomys*, is dominated by the murines *Apodemus atavus* and *Castillomys*. In contrast to the Teruel Basin, only one *Stephanomys* lineage (*S. donnezani – thaleri*) is present and the proportion of *Trilophomys* is low. Likewise, the single representative fauna from the most western basin (Asta Regia 3′, Jerez Basin, Castillo and Agustí, 1996) shows the dominance of *Apodemus atavus*, *Castillomys* and *S. donnezani – thaleri* at the cost of *Dolomys*.

The age of the N15a-b boundary was based on the sequence of localities in the Villalba Alta Río - Villalba Alta composite section (Mein et al., 1990; Opdyke et al., 1997). A potential biostratigraphic discrepancy characterizes the transitional sequence, however, with VA2 (3.92 Ma) containing N15a species *Mimomys davakosi* and VA4 (4.01 Ma) containing N15b species *Dolomys adroveri* (see Section 4.4.2; Table S4, Appendix A), implying an alternation of the two arvicoline species during this short interval. As a conservative solution, we bracket the N15a-b boundary between 4.01 Ma and 3.92 Ma. The marine Zanclean-Piacenzian boundary (3.60 Ma) correlates to the middle part of Zone N15b.

The *Mimomys hassiacus-polonicus* lineage replaces *Dolomys* in the ***Mimomys hassiacus* Zone** (**Ib-N16a**, early Villanyian, early Piacenzian) in the Teruel Basin, where arvicolines replace murines as the dominant group. *Stephanomys (S. donnezani – thaleri)* remains important in the Guadix-Baza Basin.

Based on Oms et al.'s (1999) magnetostratigraphic reinterpretation of Opdyke et al.'s (1997) results for the Escorihuela Section in the Teruel Basin, the age of the N15b-16a boundary is constrained to lie between Escorihuela B (3.19 Ma, N15b, with *Dolomys adroveri*) and Escorihuela/Escorihuela A (3.11 Ma, N16a, with *Mimomys hassiacus*; see also Section 4.3.3). A third level, Escorihuela C (3.16 Ma) can be regarded as a 'boundary fauna', because it lacks both *Dolomys* and *M. hassiacus* (but contains *M. gracilis*). (Mein et al. (1990), on the other hand, consider Escorihuela C to belong to the 'Zone à *M. gracilis* + *M. hajnackensis*', which is equivalent to N16a.) The magnetostratigraphically inferred age of 3.18 Ma for N16a site Zújar 10 in the Guadix-Baza Basin can be used to significantly narrow down the boundary to 3.19–3.18 Ma. Although ZU10 does not contain *Mimomys hassiacus*, it contains *M.* cf. *polonicus*, which is viewed as its temporal successor (Oms et al., 1999; Piñero et al., 2018). (We also note that the presence of *Mimomys* cf. *polonicus* in the Guadix-Basin pre-dates its presence in the Teruel Basin, where it is associated with *Kislangia ischus* in local Zone O4, which correlates to N16b.)

The addition of the large-sized arvicoline *Kislangia ischus* marks the transition to the ***Kislangia ischus* Zone** (**Ib-N16b**, late Villanyian, late Piacenzian). In the Teruel Basin, the medium-sized *M. hassiacus-polonicus* lineage remains dominant, while in the Guadix-Baza Basin this position is filled by the smaller-sized *Mimomys gracilis-stehlini* lineage, with the *Stephanomys donnezani – thaleri* still being well-represented (35%).

The N16a-16b boundary (3.05 Ma) is constrained between 3.06 Ma, the age of Gea 0 (Teruel Basin, N16a, see Section 4.4.2) and 3.03 Ma, the age of Zújar 11 (Guadix-Baza Basin, N16b; Oms et al., 1999).

The highest two Zones are only represented quantitatively in the Guadix-Baza Basin. In the ***Mimomys medasensis* Zone** (**Ib-N17a**, late Villanyian, Gelasian), arvicolines now also reach dominance in the South, where they are especially well represented by the name-giving species. *Kislangia* is represented by *K.* aff. *cappettai* and *K. gusii*.

The N16b-17a boundary is constrained to lie between 2.56 Ma (Concud Estación 2, Teruel Basin) and 2.54 Ma. The latter age stems from our re-interpretation of the Valdeganga section with an inferred age of 2.54 Ma for N17a level Valdeganga I (Section 4.4.2). The age of 2.44 Ma for N17a site Galera G (Guadix-Baza Basin; Garcés et al., 1997) is consistent with this interpretation. The N16b-17a boundary slightly post-dates the Pliocene-Pleistocene boundary and marine Piacenzian-Gelasian boundary (2.58 Ma).

The transition to the ***Mimomys realensis* Zone** (**Ib-N17b**, latest Villanyian, Gelasian-Calabrian transition) is associated with another expansion of arvicolines at the cost of *Stephanomys*. Other arvicolines besides *M. realensis* (a form that probably includes *M.* 'cf. *reidi*') reported from the Guadix-Baza Basin are *M.* aff. *pliocaenicus* (descendant of *M. polonicus*) and *Kislangia* aff. *cappettai*.

According to the magnetostratigraphic results of Garcés et al. (1997) for the Galera section (Baza Basin) the N17a-b boundary is situated between Galera 2 (2.25 Ma) and Galera H (1.98 Ma). Furthermore, the magnetostratigraphic correlation of N17a site Villarroyo (La Rioja) to a position in the Reunion chron (C2r.1r-1n; 2.155–2.120 Ma; Pueyo et al., 2016) implies a maximum age of 2.15 Ma for Zone N17b. Using the lithostratigraphic correlation of Alquería (N17b) to the Galera section (Oms et al., 2000), the upper boundary can be lowered to 2.04 Ma. Although an alternative interpretation of the upper part of the Galera section was put forward by others (Scott et al., 2007), our re-interpretations of the Valdeganga section (Júcar Basin; Mein et al., 1978; Opdyke et al., 1997; Section 4.4.2) and Fuentenueva section (Guadix-Baza Basin, Scott et al., 2007) confirm the original Galera ages, with a minimum age of 2.11 Ma for N17a/b transitional level VDG-II, and an age of 2.05 Ma for N17b site Fuentenueva 1. Combining all information, the uncertainty interval for the N17a-b boundary can be set to 2.15–2.05 Ma.

The top of the N17b Zone is chosen to coincide with the entry of rootless voles, a widespread event commonly used to define the Villanyian-Biharian boundary (e.g., Tesakov, 1998). Whereas *Allophaiomys* is generally considered to be the first rootless form to enter Europe, also other rootless forms (in *Mimomys*) have been found in similarly aged sediments in the Guadix-Baza Basin (Agustí, 1998; Oms et al., 2000). Given the diverging opinions on local Guadix-Baza Basin stratigraphy (Oms et al., 2000, Scott et al., 2007), we refrain from making a final calibration of these sedimentary sequences to the GPTS (Orce section; see Suppl. Text, Appendix A). Instead, we use the western European correlation of the *Allophaiomys* event to the Olduvai chron (C2n, 1.93–1.78 Ma) or just before (Repenning et al., 1990; Maul and Markova, 2007). For the Iberian domain, the implied maximum age of ~2.0–1.8 Ma for the top of Ib-N17b can be further reduced to 1.90–1.8 Ma, given our estimated age of 1.90 Ma for N17b site Valdeganga IV (see Section 4.4.2).

4.4. Chronology of sections and sites

4.4.1. Tortonian-Messinian transition

The chronology of the Tortonian-Messinian transition interval in Spain was refined using (*i*) the new stratigraphical results in

the Jumilla-La Celia and Teruel Basins, and (*ii*) the ages of Iberian Zone boundaries Ib-N11-12a and N12a-12b.

The magnetic polarity pattern of the combined La Celia and Los Barracones sections shows three reversed and two normal polarity intervals (Figs. 4 and 5). In addition, two very short normal polarity magnetozones were identified in the La Celia section at 42 m and 56 m. Whether these represent true geomagnetic features or artifacts of the sediment remanence acquisition remains unknown to us. But given their short thickness, their relevance for correlation with the GPTS is negligible since the time scale may be incomplete for very short geomagnetic chrons.

Especially the La Celia site is biostratigraphically relevant (van Dam et al., 2014). Although the exact spot of the La Celia site could not anymore be recovered, its position directly N of the main road near the road junction in the La Celia village (Agustí et al., 1985: their Fig. 7) leaves only one serious option for its stratigraphic position as the one corresponding to a brown-colored (relatively organic-rich) mudstone horizon ~5 m above the present main road (at 85 m in Fig. 4(E)). (Lower and higher levels are reddish-colored and presumably barren.) With the *Parapodemus meini – Castromys littoralis* lineage present, La Celia belongs to the *Parapodemus meini* Zone (Ib-N12b). By contrast, the lower positioned sites of Los Gargantones, which contain *Huerzelerimys turoliensis* and *Parapodemus barbarae*, belong to the lower *Huerzelerimys turoliensis* Zone (Ib-N12a).

Based on the polarity pattern alone, three options for the correlation to the GPTS should be considered (Fig. 4(F)):

I. Correlation of N1 to C3Br.2n and of N2 to C3Br.1n. The pattern of two short normal intervals separated by a longer reversed fits the equivalent pattern in the GPTS. On the other hand, a strong increase in sedimentation rate (or hiatus) must be assumed to explain the absence of a third normal interval in the upper part that would be equivalent to C3Bn;
II. Correlation of N1 to C3Br.2n (as in option I) and of the top of N2 to the top of C3Bn. The long, reversed interval conveniently correlates to C3Ar, but either C3Br.1n or C3Br.1r is missing;
III. Correlation of the base of N1 to the base of C4n.1n and the top of N2 to the top of C3Bn (as in option II). This option is in accordance with the substantial length of N1 in the JCBA section, which seems too long to correspond to C3Br.2n. This latter chron or CrBr.3r is missing.

In order to choose between the three magnetostratigraphic options, we additionally make use of (*i*) the time-equivalent record in the Teruel Basin, and (*ii*) biochronology based on molar size.

Magnetostratigraphic option I for the JCLC and JCBA sections implies an age of 7.26 Ma for N12b site LCE, which at the same time functions as a minimum age for N12a site CC3, positioned at cycle 18 in the CCLP section (Fig. 4(A, E)). The presence of ~17 cycles (~350kyr) between N12a sites CCB/CCL and CC3 implies a minimum age of ~7.60 Ma for the former, in agreement with the age of 7.68–7.65 Ma for the Ib-N11-12a boundary as established in the Cabriel Basin (Opdyke et al., 1989, 1997; Table S4, Appendix A). While option I leaves ~0.04 myr (three precession cycles, Fig. 4 (E)) for the exact placing of the Las Pedrizas section, options II and III leave more space to accommodate the section given a younger age of 7.09 Ma for Ib-N12b site LCE. As will be shown in section Section 4.4.4, these options also allow several other N12a localities that are younger than CC3 to be properly placed.

Although a more detailed sedimentological study of the observed small-scale cycles would be necessary to establish a final interpretation ('tuning') of the Las Pedrizas section, the following correlations can be hypothesized from a chronostratigraphic point of view (Fig. 4(F)):

- The association of the featureless middle part (which we take to include cycles 13–21) to the interval encompassing nine precession minima with reduced amplitude corresponding to the 400-kyr/2.4-myr eccentricity minimum between 7.4–7.2 Ma;
- The correlation between a possible deepening starting in cycle 13 (end of interval with lignite streaks and root structures, laminar microstructure in thin section LP0-1) with the transition towards the first low-amplitude precessional minimum at 7.386 Ma;
- The correlation of a possible shallowing starting in cycle 21–22 (reduced lamination, increase in the amount of well-preserved gastropod fragments, and the appearance of palustrine features in the form of microscopic cracks and indurated bed tops) with an interval of more extreme precessional minima starting at 7.190 Ma.

The best match of the cyclostratigraphic pattern to the precessional curve is the one in which the middle, deeper part is taken maximally, i.e., including cycle 13 (instead of 14) and including transitional cycle 21 (as counted in Fig. 4(E), i.e., with four cycles in the 'non-exposed' interval). Downward counting of cycles yields an age of 7.657 Ma for cycle 1 (precession minimum) and Ib-N12a localities CCL/CCB, i.e., just within the Ib-N11-12a boundary uncertainty range as inferred in the Cabriel Basin (7.68–7.65 Ma; Table S4, Appendix A). Downward extrapolation (using the same sedimentation rate) yields an age well into long normal chron C4n.2n (7.73 Ma) for the uppermost normal sample in the CCCG section. We can therefore safely assume that our polarity interval N corresponds to chron C4n.2n (Fig. 4(E)).

Because of the various cyclostratigraphic uncertainties, we will allow the whole sequence to be placed 1 or 2 precession cycles higher (Fig. 4(E)). As will be discussed in Section 4.4.4, the resulting minimum age for the youngest Teruel Basin N12a locality still predates the next higher (Ib-N12a-b) Zone boundary. On the other hand, a lower placement by one cycle would imply an age of 7.675 Ma for the CCL/CCB localities (cycle 1), which is older than the allowed minimum age of 7.66 Ma for a N12a site (given the age of 7.68 Ma for N11 site Balneario and maximum age of 7.67 Ma for N11-12a boundary site Crevillente 4; see next Section).

4.4.2. Magnetostratigraphic updates of Teruel and Júcar Basins

Besides the major update for the Tortonian-Messinian transition, several smaller updates to the Iberian magnetostratigraphic framework were performed (Table S4, Appendix A). The first two represent combinations of previously published results, the third involves new/revised correlations of individual sites to existing polarity patterns, whereas the last update combines previous paleomagnetic and faunal results with a newly inferred regional zone boundary age:

1. The correlation to the GPTS of the polarity pattern of the upper part of the Late Miocene **El Búnker section** (Teruel Basin; Krijgsman et al., 1996; van Dam et al., 2001) is confirmed by more recent work in the Cabriel Basin (Gibert et al., 2013). The latter work includes an age estimate for key site Venta del Moro that is incompatible with younger options for the Teruel Basin polarity pattern;
2. Opdyke et al. (1997) discussed two options (C2An.1n or C2An as a whole) for the correlation of the upper normal interval in the Late Pliocene **Gea section** in the Teruel basin. The second option can be eliminated, however, given the magnetochronologic reinterpretation of the nearby Escorihuela section (Oms et al., 1999);
3. Teruel Basin sites Villalba Alta Río 1–4, Villalba Alta 5, Orrios 1, 3 and 4 were previously correlated to the GPTS based on polarity patterns as recorded in the **Villalba Alta Río - Villalba Alta**

composite and **Orrios** (ORR) **sections** (Opdyke et al., 1997). Here, we use the lithostratigraphic schemes from Mein et al. (1990: their Figs. 4 and 5) to correlate sites Villalba Alta 1–4, Orrios 7, and Orrios 9C to the main sections (and hence to the GPTS) as well. Secondly, ages of Escorihuela/Escorihuela A and Escorihuela B in the Late Pliocene **Escorihuela section** of van Dam et al. (2006) are slightly modified based on the combined stratigraphic information in Mein et al. (1990) and Opdyke et al. (1997). Thirdly, locality ages for the nearby **Concud-Estación** section (Opdyke et al., 1997) are estimated on the basis of the sedimentation rate for C2An.1n as recorded in the nearby Gea section

4. The magnetostratigraphic correlation of the **Valdeganga section** in the Júcar Basin to the GPTS (Opdyke et al., 1997) is re-interpreted in the light of more recent paleomagnetic results in the Guadix-Baza Basin (Oms et al., 1999), which, in combination with update 2 above, results in an 3.06–3.03 Ma age range for the N16a-b boundary. Given this range, the lowest levels of the Valdeganga section (Valdeganga 14–15, N16b) should correlate to C2Ar.1n (3.03–3.58 Ma; Fig. 7). The remaining part of the Valdeganga section, which mostly consists of samples of reversed polarity, thus correlates to C2r (Matuyama chron; in accordance with the interpretation of Opdyke et al., 1997). Based on an upward extrapolation of the sedimentation rate, an age of 1.92 Ma for the uppermost normal sample (i.e., within the Olduvai chron, C2n, 1.95–1.78 Ma) and 1.90 Ma for the uppermost N17b mammal site Valdeganga IV is estimated.

4.4.3. Sections without first-order correlation to the GPTS

Several sections in the Bajo Segura, Granada, Alcoy, and Teruel Basin lack first-order magnetostratigraphic control, but can be dated by combining regional biostratigraphy with local sedimentation rates. A summary of the results is presented below. (Details can be found in the Suppl. Text and Table S4, Appendix A, which includes age-depth calculations.).

Although the **Crevillente section** (which consists of the Castro and Crevillente Dam sections; de Bruijn et al., 1975; Freudenthal et al., 1991) in the Bajo Segura Basin has no magnetostratigraphic record, locality ages can be constrained by combining stratigraphic heights (Martín-Suárez and Freudenthal, 1998) with ages of zone boundaries (between N11, 12a, 12b, 13a and 13c). With the N11b-12a boundary constrained to 7.68–7.65 Ma, the minimum age for N12b to 6.89 Ma, and the maximum age for N13c to 6.25 Ma, ages ranges for sites can be estimated assuming a constant rate of sedimentation. This procedure results in an average locality age uncertainty of 0.19 myr (Table S4, Appendix A). The age estimate of 7.02–6.89 Ma thus inferred for N12b site Crevillente 17 adds in constraining the maximum age for N13a locality BUN in the **El Búnker section** (Teruel Basin) to 7.00 Ma. (Because of a low paleomagnetic sampling density and sedimentation rate, considerable uncertainty in maximum and minimum age for El Búnker and El Búnker 4/5 was inferred by allowing chron boundary levels to vary between bracketing paleomagnetic samples (Table S4, Appendix A).)

The locality **Crevillente 4** (de Bruijn et al., 1975), which was not included in later systematic papers by Freudenthal, Martín-Suárez and colleagues, is relevant from a stratigraphic point of view because of its transitional character. While *Occitanomys* size in this site is like that of *O. sondaari* from its N11 type population Tortajada A, the murine composition is atypical, with *Parapodemus* entirely represented by *P. gaudryi*, a form only marginally present in N11 in the Teruel Basin (e.g., Los Aguanaces 3; van Dam, 1997) and even more rarely present in Zone N12a (van Dam et al., 2001, 2014). Our re-inspection of the cricetine species named '*Kowalskia* aff. *fahlbuschi*' by de Bruijn et al. (1975) in Crevillente 4, revealed a morphological stage intermediate between *Neocricetodon occidentalis* (typical for N11) and *Apocricetus* (aff.) *plinii*, (typical for N12a, but with some occurrences in N11 as well). Although the correlation of Crevillente 4 to the composite section of Martín-Suárez and Freudenthal (1998) has turned out to be complicated lithostratigraphically (Freudenthal et al., 1991), the site can be biostratigraphically placed between Cabriel Basin sites Balneario (N11, 7.68 Ma) and Fuente Podrida (N12a, 7.65 Ma) (see also Suppl. Text, Appendix A).

The **Arenas del Rey section** in the SW part of the Granada Basin contains 15 localities (series of La Mina, La Dehesa and Calerico; Boné et al., 1978; Padial-Ojeda, 1986; García-Alix et al., 2008a) of which the large majority belongs to Zones N13b-c. The highest site (La Dehesa D5; Boné et al., 1978) contains *Celadensia* as a rare element (Castillo et al., 1990) and is accordingly assigned to N14a. By varying the position of the N13b-c and N13c-14a boundaries between locality levels, age ranges for all sites can be estimated under the assumption of a constant sedimentation rate. This procedure resulted in an average age uncertainty of 0.14 myr. Furthermore, magnetobiostratigraphic work in the **Purcal section** in the northeastern part of the basin (Martín Suárez et al., 1998) has shown that the three superposed sites Purcal 3 (N13c), Purcal 4 and Purcal 7 (both N14a) are all positioned in a reversed chron, for which the only viable option is C3r (6.02–5.24 Ma). Age ranges for these sites were constructed using the age range of 5.47–5.33 Ma for the N13c-14a boundary and assuming a constant sedimentation rate between 10–40 cm/kyr (this latter range was conservatively chosen given observed rates of ~ 20–25 cm/kyr in nearby lacustrine successions; Fernández and Soria, 1996).

Mansino et al. (2017) presented the stratigraphic positions of 16 sites near **Alcoy**. The sequence starts with the sites of Alcoi Forn, which can be assigned to N13c-14a, and which are overlain by the main section of Gormaget Ravine, containing sites belonging to N14b. The uppermost sites Alcoi 2C/2D can be assigned to N14c based on the presence of *Stephanomys cordii* and *Apocricetus* cf. *angustidens*. By varying the ages of the N14a-b, N14b-c and N14c-15a boundaries between their minimum and maximum values and assuming a constant rate of sedimentation, age ranges for all sites could be estimated. The average uncertainty amounts to 0.17 myr.

The **Lomas de Casares section** in the Teruel Basin (Mein et al., 1990) contains 'middle Turolian' (i.e., potentially N12a-b) levels (Barranco de Cuevas 1–4) in its basal part, and N14a (Lomas de Casares 2/5, 3) and N15a (Lomas de Casares 1) sites in its upper part. The age of latter site can be constrained biochronologically to lie between the magnetostratigraphically constrained ages of Villalba Alta 3 (4.15 Ma) and 1 (4.04 Ma). On the basis of a maximum age of 7.67 Ma for the Barranco de Cuevas sites, a maximum age of 4.14 Ma for Lomas de Casares 1, a minimum age of 4.87 Ma for Lomas de Casares 2/5 (because older than N14b site La Bullana 3), and the assumption of a constant sedimentation rate in the Lomas de Casares section, an age range of 5.20–5.07 Ma for Lomas de Casares 3 is calculated, which is consistent with the inferred maximum age range for N14a (5.46 Ma). The above calculations partly depend on the correlation of the Ib-N14b sites of **La Bullana** (3 and 2B) to C3n.3n and C3n.2r, respectively. As further explained in the supplementary text (Appendix A), we regard a still younger correlation of the La Bullana sites to C3n.2n and C3n.1r (Piñero and Agustí, 2020) unlikely, as it is incompatible with the age of the N14b-c boundary as defined by the age of boundary fauna Sifón de Librilla P.

4.4.4. Localities with ages inferred from evolutionary rates

No tooth element category successfully passed both the 'zone test' and 'superposition test' using the combined data for the three zones Ib-N12a, 12b and 13c (for data and analysis, see Table S5, Appendix A). However, when the data were confined to N12a

(which contains most sites), the sequence of M1 average length measurements ($n \geq 10$) passed both tests (Table S5, Appendix A). (Lowering the sampling threshold to $n \geq 5$ allowed more localities to be included but led to violations in both tests.) Whereas the plot of M1 length against calibrated age showed a monotonously increasing trend, trends in other elements (M2, m2, and to a lesser degree m1) as well as in the first principal component PC1 of all four size variables, showed a more erratic pattern including a strong size difference around 7.5 Ma. (Fig. S4, Appendix A). Such an increase is difficult to explain given the overall taxonomic stability across the whole zone.

The more irregular trend in second molars could be related to their larger natural variability. In his study of the lower dentition in 17 different mammal groups, Gingerich (1974) showed that within-population size is the least variable in first molars, the possible reason being their early development preventing the expression of sexual dimorphism. In their review of upper and lower tooth length and width variation in Cenozoic European hamsters and true mice, Freudenthal and Cuenca Bescos (1984) and Freudenthal and Martín-Suárez (1990) find the lowest variation in M1, m1 and m2 length. Additional variability in M2 in murines could be due to the large difference in measured occlusal length between worn and unworn specimens and/or to the use of slightly different conventions regarding orientation (e.g., compare van de Weerd (1976) and Martín-Suárez and Freudenthal (1993)). Here, we opted for M1 length as our final metric for age inter- and extrapolation. This choice differs from the one in van Dam (1997), who applied a measure based on all four elements (principal component 1, PC1) to a more restricted set of sites.

Four Ib-N12a sites (Los Mansuetos, Concud Cerro de la Garita 5, Tortajada and Aljezar B) have a larger *Occitanomys adroveri* M1 size than Concud 3 (CC3), the highest locality in the cyclostratigraphically calibrated Concud series (see Section 4.4.1). Because the lowermost CCB/CCL level only contains seven measurable *O. adroveri* M1, we used CCCG (7.57–7.52 Ma, n = 20) and CC3 (7.28–7.24 Ma, n = 57) as our primary calibration points for further age inter- and extrapolation (Table 3). As a result, three of the four above mentioned sites have predicted ages of 7.27-7.26 Ma, whereas the estimated age for Aljezar B is clearly younger (7.18–7.14 Ma). A similar result is implied by the size of M2, which also points to Aljezar B as clearly being the youngest N12a site (Table S5, Appendix A). We therefore conclude that magnetostratigraphic option I for the Jumilla-La Celia Basin (implying a minimum age of 7.27 Ma for N12a) is not the most probable option. The rejection of option I implies that the short reversed chron C3Br.3r is not recorded, and that N1 represents an amalgamation of C4n.1n and C3Br.2n. In choosing between options II and II, we prefer the former, given the substantial length of interval N1 in the Los Barracones section.

The application of the 'best-fit' cyclostratigraphic scenario for the Las Pedrizas section (see Section 4.4.1), which at the same time represents the oldest possible solution, leads to a secondary inconsistency with regard to N12a level Tortajada C/D, for which a size-based age range of 7.70–7.65 Ma is estimated (Table 3), which partly exceeds the maximum age of 7.68 Ma for the N11-N12a boundary. Moreover, an even older age for Ib-N12a locality Tortajada B follows from its position ~ 7 m below Tortajada C/D (van Dam et al., 2001). Statistical error may play a role, because the latter level just contains the minimum required amount of 10 specimens. Other elements (m1, m2) appear to point an age younger than that of Crevillente 15, which is constrained to maximally 7.61 Ma on the basis of sedimentation rates (see Section 4.2.3). Because we give priority to the sedimentation rate method over the size-based method, while accepting 7.61 Ma as a maximum, the average age of Tortajada C/D is (slightly arbitrarily) set to 7.61 Ma as well (7.63–7.58 Ma), thereby leaving space to accommodate lower site Tortajada B within N12a (set at 7.66–7.61 Ma). An age close to the N11-12a boundary of the Tortajada sites is consistent with the virtual absence of the hamster *Hispanomys* (only one specimen in Tortajada C), a feature shared with the other basal N12a sites CCB and CCL (7.66–7.62 Ma). The extension of the range of the typical N11 hamster *Neocricetodon occidentalis* into the basal part of N12a (CCL; see Suppl. Text, Appendix A) also points to a short transitional stage in the hamster community around the N11-12a boundary. This transition is time-equivalent to the remarkable change in the true mice community as recorded across the N11-12a boundary and in transitional fauna Crevillente 4 (see Section 4.4.3).

The age of 7.27–7.22 Ma as predicted for CG5 based on molar size implies the presence of a hiatus between CCCG (7.57–7.52 Ma) and CG5 (Fig. 4(E)). A period of non-deposition is feasible given the position of the section close to the Mesozoic basement (Fig. 3) in combination with a rather heterogeneous lithology in the upper part of the section (including white and grey nodular limestones, lignitic clays and grey marls).

We additionally examined the possibilities of using size increase in the long-lasting lineage *Stephanomys ramblensis* – *S.*

Table 3
Size-based age estimations for localities with ten or more M1 of *Occitanomys adroveri*, using cyclostratigraphically inferred ages for CG5 and CC3 as tie points.

Locality	Code	Basin	Ib-Zone	Tie points (Ma)		Mean L(M1)	N	Size-based age (Ma)		Reference measurements
				max.	min.			max.	min.	
Valdecebro 5	VDC5	Teruel	N12b			2.100	32			Adrover et al. (1986)
Crevillente 14	CR14	Bajo Segura	N13a			2.094	13			Martín-Suárez and Freudenthal (1993)
Crevillente 17	CR17	Bajo Segura	N12b			2.080	48			Martín-Suárez and Freudenthal (1993)
Los Aljezares B	ALJB	Teruel	N12a			2.060	80	7.18	7.14	Adrover (1986)
La Roma 5A	R5A	Teruel	N12b			2.044	14			this paper
Tortajada	TO	Teruel	N12a			2.039	17	7.26	7.22	van de Weerd (1976)
Concud Cerro de la Garita 5	CG5	Teruel	N12a			2.037	10	7.27	7.22	this paper
Los Mansuetos	LM	Teruel	N12a			2.036	68	7.27	7.23	van de Weerd (1976)
Concud 3*	CC3	Teruel	N12a	7.283	7.242	2.032	57	7.28	7.24	van de Weerd (1976)
La Roma 5B	R5B	Teruel	N12a			1.994	23	7.42	7.38	this paper
Masada del Valle 5	MDV5	Teruel	N12a			1.988	24	7.44	7.40	van de Weerd (1976)
Cubla 2	CU2	Teruel	N12a			1.962	30	7.53	7.49	Besems and van de Weerd (1983), this paper
Villalba Baja 2	VB2	Teruel	N12a			1.954	18	7.56	7.52	van de Weerd (1976); this paper
Concud Cerro de la Garita*	CCCG	Teruel	N12a	7.570	7.524	1.952	20	7.57	7.52	van de Weerd (1976); this paper
Casa del Acero	ACERO	Fortuna	N12a			1.950	20	7.58	7.53	Agustí et al. (1981)
Masada del Valle 2	MDV2	Teruel	N12a			1.938	69	7.62	7.57	van de Weerd (1976)
Crevillente 15	CR15	Bajo Segura	N12a			1.933	24	7.64	7.59	Martín-Suárez and Freudenthal (1993)
Tortajada C/D	TOC/D	Teruel	N12a			1.917	10	7.70	7.65	van de Weerd (1976); this paper

* Used for calibration.

dubari – S. cordii – S. margaritae – S. vandeweerdi – S. minor – S. prietaensis – S. balcellsi – S. 'progressus' (Adrover, 1986) for dating sites belonging to the latest Miocene (Zones N13a,b,c) and Pliocene (mostly data from Zones 14a-b). Upper first molars were selected in order to include the four calibrated sites Sifón de Librilla 3, 61, P, and Venta del Moro (which all contain eight M1, which is more than the frequency of other elements). After compiling data for 21 sites, the size ranking of localities suffered from violations of the zone test, with size values in southern basins often being lower than in the Teruel Basin (not shown). Furthermore, as shown in the case of *Occitanomys*, the method can be assumed to work best within zones (i.e., within the context of a relatively stable community). Unfortunately, in the case of *Stephanomys*, no zone satisfied the combined requirement of a sufficient number of specimens and a minimum of two calibrated tie points for the size-based approach to be successfully applied.

Finally, locality rankings based on molar size trends in another potentially suitable lineage, *Apodemus gudrunae – A. gorafensis* (N13a-15a) yielded too many zone inconsistencies in order to be reliably used for chronological purposes. Local differences could have played a role here given the relatively early (Zone '13a') appearance of *A. gorafensis* in the Fortuna Basin (Piñero and Agustí, 2019), casting some doubts on the validity of a simple ancestor–descendant relationship (Martín-Suárez and Mein, 1998; García-Alix et al., 2008b).

4.4.5. Remaining localities

Age ranges for localities that could not be constrained by sedimentary or evolutionary rates were taken maximally with regard to the (maximum) age range for their zone or faunal stage (for an overview of sites per basin, see Suppl. Text, Appendix A).

5. Conclusions

A review of 8.5–2 Ma-old rodent faunas and calibrated sections across the Iberian Peninsula has resulted in a new regional biozonation with estimated age uncertainty ranges for boundaries and micromammal sites. Although the magnitude of between-zone turnover differs from boundary to boundary, approximate isochrony for most Iberian Zone boundaries is suggested by shared relative abundance patterns for both the faunal assemblages and their turnover. New stratigraphic and paleontological data for the Tortonian-Messinian transitional interval (8–7 Ma) in the Teruel and Jumilla – La Celia Basin have significantly improved the age control for this thus far poorly calibrated interval on the Iberian Peninsula.

Declaration of Competing Interest

The authors declare that they have no known competing financial interests or personal relationships that could have appeared to influence the work reported in this paper.

Acknowledgments

We dedicate this paper to Hans de Bruijn, who sadly passed away in 2021. Hans was one of the founding fathers of micromammal paleontology and a principal initiator of systems of rodent-based biostratigraphy in Spain and many other areas. We thank Raef Minwer Barakat for allowing us to use his quantitative data for Guadix-Baza Basin rodents, Everett Lindsay for his information on the lithostratigraphy of sections in the Teruel Basin, and Plinio Montoya for his help in clarifying the stratigraphy of La Bullana. We thank Alexey Tesakov for sharing his insights on *Dolomys* and other arvicoline lineages. We acknowledge Karel Steensma for his invaluable help during the various field campaigns, and Lorenzo Vilas and Cayetano Herrero for discussions during field work in the La Celia area. Eduardo Espílez and Luis Mampel are thanked for taking rock samples for sedimentology, and João Trabucho, Jose Pedro Calvo and Ana Alonso for their help in characterizing the sedimentary paleoenvironment of the Las Pedrizas section, Anita van Leeuwen for carrying out XRD analyses at Utrecht University, Dolors Barsó for preparing the thin sections at the Faculty of Earth Sciences at University of Barcelona, and Jasper Huijsmans for his assistance with microscopy. We thank the three reviewers for their comments and Frits Hilgen for his valuable feedback regarding the structure of the manuscript and the Teruel Basin cyclostratigraphy. This work was funded by MCIN/AEI/10.13039/501100011033 (R + D + I project PID2020-117289GB-I00), AEI-FEDER EU (to M.F.), AGAUR (Consolidated Research Group, 2017 SGR 960 to M.F. and 2017 SGR 596 to M.G.), the Generalitat de Catalunya/CERCA Program (to J.A.v.D. and M.F.), and the Department of Science, University and Society of Knowledge of the Government of Aragon (Reference Research Group E04_20R FOCONTUR funding to Fundación Dinópolis-L.A.). We also thank the support of Department of Education, Culture and Sport of the Government of Aragon, and its General Directorate of Cultural Heritage for the permissions to excavate in several paleontological sites of Teruel.

Appendix A. Supplementary material

Supplementary information (including Suppl. Text, Figs. S1-S4 and Tables S1-S5) associated with this article can be found, in the online version, at: https://doi.org/10.1016/j.geobios.2023.01.001.

References

Abdul Aziz, H., van Dam, J.A., Hilgen, F., Krijgsman, W., 2004. Astronomical forcing in Upper Miocene continental sequences: implications for the Geomagnetic Polarity Time Scale. Earth and Planetary Science Letters 222, 243–258.

Abels, H.A., Abdul Aziz, H., Calvo, J.P., Tuenter, E., 2009a. Shallow lacustrine microfacies document orbitally paced lake-level history in the Miocene Teruel Basin (NE Spain). Sedimentology 56, 399–419.

Abels, H.A., Aziz, H.A., Ventra, D., Hilgen, F.J., 2009b. Orbital climate forcing in mudflat to marginal lacustrine deposits in the Miocene Teruel Basin (Northeast Spain). Journal of Sedimentary Research 79, 831–847.

Adrover, R., Alcalá, L., Mein, P., Moissenet, E., Orrios, J., 1986. Mamíferos del Turoliense medio en la Rambla de Valdecebro, Teruel. Estudios Geológicos 42, 495–509.

Adrover, R., Mein, P., Moissenet, E., 1993. Roedores de la transición Mio-Plioceno de la región de Teruel. Paleontologia i Evolució 26–27, 47–84.

Adrover, R., 1986. Nuevas faunas de roedores en el Mio-Plioceno continental de la región de Teruel (España). Interés bioestratigrafica y paleoecologico. Instituto de Estudios Turolenses de la Excma. Diputacion Provincial de Teruel, Teruel.

Agustí, J., 1998. A review of Late Pliocene to Early Pleistocene arvicolid evolution in Spain. Paludicola 2, 8–15.

Agustí, J., Gibert, J., Moyà-Solà, S., 1981. Casa del Acero; Nueva fauna turoliense de vertebrados (Mioceno superior de Fortuna, Murcia). Butlleti Informatiu - Institut de Paleontologia de Sabadell 13, 69–87.

Agustí, J., Moyà-Solà, S., Gibert, J., Guillén, J., Labrador, M., 1985. Nuevos datos sobre la bioestratigrafía del Neógeno continental de Murcia. Paleontologia i Evolució 18, 83–93.

Agustí, J., Cabrera, L., Garcés, M., Krijgsman, W., Oms, O., Parés, J.M., 2001. A calibrated mammal scale for the Neogene of Western Europe; State of the art. Earth-Science Reviews 52, 247–260.

Agustí, J., Garcés, M., Krijgsman, W., 2006a. Evidence for African-Iberian exchanges during the Messinian in the Spanish mammalian record. Palaeogeography, Palaeoclimatology, Palaeoecology 238, 5–14.

Agustí, J., Oms, O., Furió, M., Perez-Vila, M.J., Roca, E., 2006b. The Messinian terrestrial record in the Pyrenees: the case of Can Vilella (Cerdanya Basin). Palaeogeography, Palaeoclimatology, Palaeoecology 238, 179–189.

Alcalá, L., 1994. Macromamíferos Neógenos de la Fosa de Alfambra-Teruel. Instituto de Estudios Turolenses - Museo Nacional de Ciencias Naturales, Teruel.

Alcalá, L., van Dam, J.A., Luque, L., Montoya, P., Abella, J., 2005. Nuevos mamíferos vallesienses en Masía de La Roma (Cuenca de Teruel). Geogaceta 37, 199–202.

Alcalá, L., Luque, L., van Dam, J.A., Rubio, J.C., 2018. Cuenca de Teruel y Fosa del Jiloca. In: Alcalá, L., Calvo, J.P., Simón, J.L. (Eds.), Geología de Teruel. Instituto de Estudios Turolenses, Teruel, pp. 99–129.

Alonso-Zarza, A.M., Calvo, J.P., 2000. Palustrine sedimentation in an episodically subsiding basin: the Miocene of the northern Teruel Graben (Spain). Palaeogeography, Palaeoclimatology, Palaeoecology 160, 1–21.
Alonso-Zarza, A.M., Meléndez, A., Martín-García, R., Herrero, M.J., Martín-Pérez, A., 2012. Discriminating between tectonism and climate signatures in palustrine deposits: Lessons from the Miocene of the Teruel Graben, NE Spain. Earth-Science Reviews 113, 141–160.
Álvarez Sierra, M.A., Daams, R., Lacomba, J.I., López-Martínez, N., Sacristán-Martín, M.A., 1987. Succession of micromammal faunas in the Oligocene of Spain. Münchener Geowissenschaftliche Abhandlungen A 10, 43–48.
Anadón, P., Moissenet, E., Simón, J.L., 1990. The Neogene grabens of the Eastern Iberian Caín (eastern Spain). Paleontologia i Evolució, Memória Especial 2, 99–130.
Besems, R.E., van de Weerd, A., 1983. The Neogene rodent biostratigraphy of the Teruel-Ademuz Basin (Spain). Proceedings of the Koninklijke Nederlandse Akademie van Wetenschappen, Series B 86, 17–23.
Boné, E., Dabrio, C.J., Michaux, J., Pena, J.A., Ruiz, B.A., 1978. Stratigraphie et paleontologie du Miocène supérieur d'Arenas del Rey, Bassin de Grenade (Andalousie, Espagne). Bulletin de la Societe Belge de Geologie 87, 87–99.
Castillo, C., 1990. Paleocomunidades micromamíferos de los yacimientos karsticos del Neógeno Superior de Andalucia oriental. Tesis Doctoral, Universidad de Granada, 255p.
Castillo, C., Agustí, J., 1996. Early Pliocene rodents (Mammalia) from Asta Regia (Jerez basin, Southwestern Spain). Proceedings Koninklijke Nederlandse Akademie van Wetenschappen, Serie B 99, 25–43.
Castillo, C., Freudenthal, M., Martín Suárez, E., Martínez, M.Y., Rivas, P., 1990. New localities with fossil micromammals in the Pliocene of Granada basin (Spain). Scripta Geologica 93, 41–46.
Daams, R., 1983. The dental pattern of the dormice *Dryomys*, *Myomimus*, *Microdyromys* and *Peridyromys*. Utrecht Micropaleontological Bulletins. Special Publication 3, 1–115.
Dahlmann, T., 2001. Die Kleinsäuger der unter-pliozänen Fundstelle Wölfersheim in der Wetterau (Mammalia: Lipotyphla, Chiroptera, Rodentia). Courier Forschungsinstitut Senckenberg 227, 1–129.
Daxner-Höck, G., 1980. Rodentia (Mammalia) des Eichkogels bei Mödling (Niederösterreich). 1. Spalacinae und Castoridae. 2. Übersicht über die gesamte Nagetierfauna. Annalen des Naturhistorischen Museums in Wien 83, 135–152.
de Bruijn, H., Mein, P., Montenat, C., van de Weerd, A., 1975. Corrélations entre les gisements de rongeurs et les formations marines du Miocène terminal d'Espagne méridionale; provinces d'Alicante et de Murcia. Proceedings of the Koninklijke Nederlandse Akademie van Wetenschappen, Series B 78, 282–313.
Dijksman, A.A., 1977. Georeversals as recorded in the Miocene redbeds of the Calatayud-Teruel Basin (Spain). Ph.D. Thesis, Utrecht University, 156p.
Ezquerro, L., Luzón, A., Simón, J.L., Liesa, C.L., 2020. Segmentation and increasing activity in the Neogene-Quaternary Teruel Basin rift (Spain) revealed by morphotectonic approach. Journal of Structural Geology 135, 104043.
Fejfar, O., Heinrich, W.D., Kordos, L., Maul, L.C., 2011. Microtoid cricetids and the early history of arvicolids (Mammalia, Rodentia). Palaeontologia Electronica 14, 27A.
Fernández, J., Soria, J., 1996. Evolución sedimentaria en el borde norte de la Depresión de Granada a partir del Turoliense terminal. Acta Geológica Hispanica 1996, 73–81.
Franzen, J.L., Pickford, M., Costeur, L., 2013. Palaeobiodiversity, palaeoecology, palaeobiogeography and biochronology of Dorn-Dürkheim 1 – a summary. Palaeobiodiversity and Palaeoenvironments 93, 277–284.
Freudenthal, M., Cuenca Bescos, G., 1984. Size variation of fossil rodent populations. Scripta Geologica 76, 1–28.
Freudenthal, M., Lacomba, J.I., Martín-Suárez, E., Peña, J.A., 1991. The marine and continental upper Miocene of Crevillente (Alicante, Spain). Scripta Geologica 96, 1–8.
Freudenthal, M., Martín-Suárez, E., 1990. Size variation in samples of fossil and Recent murid teeth. Scripta Geologica 93, 1–34.
Freudenthal, M., Mein, P., Martín-Suárez, E., 1998. Revision of Late Miocene and Pliocene Cricetinae (Rodentia, Mammalia) from Spain and France. Treballs del Museu de Geologia de Barcelona 7, 11–93.
Freytet, P., Verrecchia, E.P., 2002. Lacustrine and palustrine carbonate petrography: an overview. Journal of Paleolimnology 27, 221–237.
Furió, M., Agustí, J., 2017. Latest Miocene insectivores from Eastern Spain: Evidence for enhanced latitudinal differences during the Messinian. Geobios 50, 123–140.
Gamonal, A., Mansino, S., Ruiz-Sánchez, F.J., Crespo, V.D., Corbí, H., Montoya, P., 2018. Sierra del Colmenar 1A, a new late Messinian (Late Miocene) locality in the Bajo Segura Basin (SE Spain): biostratigraphic and palaeoenvironmental implications. Historical Biology 30, 380–381.
Garcés, M., Agustí, J., Cabrera, L., Parés, J.M., 1996. Magnetostratigraphy of the Vallesian (Late Miocene) in the Vallès-Penedès Basin (northeast Spain). Earth and Planetary Science Letters 142, 381–396.
Garcés, M., Agustí, J., Parés, J.M., 1997. Late Pliocene continental magnetochronology in the Guadix-Baza Basin (Betic Ranges, Spain). Earth and Planetary Science Letters 146, 677–687.
Garcés, M., Krijgsman, W., Agustí, J., 1998. Chronology of the late Turolian deposits of the Fortuna basin (SE Spain): implications for the Messinian evolution of the eastern Betics. Earth and Planetary Science Letters 163, 69–81.
Garcés, M., Krijgsman, W., van Dam, J.A., Calvo, J.P., Alcalá, L., Alonzo Zarza, A., 1999. Late Miocene alluvial sediments from the Teruel area: Magnetostratigraphy, magnetic susceptibility, and facies organization. Acta Geológica Hispanica 32, 171–184.
García-Alix, A., Minwer-Barakat, R., Martín-Suárez, E., Freudenthal, M., 2007. A late Ruscinian (Pliocene) rodent fauna from the Granada Basin (SE Spain). Journal of Vertebrate Paleontology 27, 1066–1070.
García-Alix, A., Minwer-Barakat, R., Martín-Suárez, E., Freudenthal, M., 2008a. Biostratigraphy and sedimentary evolution of Late Miocene and Pliocene continental deposits of the Granada Basin (southern Spain). Lethaia 41, 431–446.
García-Alix, A., Minwer-Barakat, R., Martín-Suárez, E., Freudenthal, M., 2008b. Muridae from the Mio-Pliocene boundary in the Granada basin (Southern Spain). Biostratigaphic and phylogenetic implications. Neues Jahrbuch für Geologie und Paläontologie Abhandlungen 248, 183–215.
Gaston, 1994. Rarity. Chapmann & Hall, London.
Gibert, L., Scott, G., Montoya, P., Ruiz-Sánchez, F., Morales, J., Luque, L., Abella, J., Lería, M., 2013. Evidence for an African-Iberian mammal dispersal during the pre-evaporitic Messinian. Geology 41, 691–694.
Gingerich, P.D., 1974. Size variability of the teeth in living mammals and the diagnosis of closely related sympatric fossil species. Journal of Paleontology 48, 895–903.
Godoy, A., Olivé, A., Moissenet, E., 1983. Mapa y memoria explicativa de la Hoja 567 (Teruel) del Mapa Geológico de España, a escala 1:50.000 (2a Serie). IGME, Madrid.
Gradstein, F.M., Ogg, J.G., Schmitz, M.D., Ogg, G., 2012. A geological time scale 2012. Elsevier, Amsterdam.
Hilgen, F.J., Lourens, L.J., van Dam, J.A., 2012. The Neogene Period. In: Gradstein, F. M., Ogg, J.G., Schmitz, M.D., Ogg, G. (Eds.), A geological time scale 2012. Elsevier, Amsterdam, pp. 923–978.
Hordijk, K., de Bruijn, H., 2009. The succession of rodent faunas from the Mio/Pliocene lacustrine deposits of the Florina-Ptolemais-Servia Basin (Greece). Hellenic Journal of Geosciences 44, 21–103.
Koufos, G.D., Vasileiadou, K., 2015. Miocene/Pliocene mammal faunas of southern Balkans: implications for biostratigraphy and palaeoecology. Palaeobiodiversity and Palaeoenvironments 95, 285–303.
Krijgsman, W., Langereis, C.G., Daams, R., van der Meulen, A.J., 1994. Magnetostratigraphic dating of the middle Miocene climate change in the continental deposits of the Aragonian type area in the Calatayud-Teruel basin (Central Spain). Earth and Planetary Science Letters 128, 513–526.
Krijgsman, W., Garcés, M., Langereis, C.G., Daams, R., van Dam, J.A., van der Meulen, A.J., Agustí, J., Cabrera, L., 1996. A new chronology for the middle to late Miocene continental record in Spain. Earth and Planetary Science Letters 142, 367–380.
Krijgsman, W., Fortuin, A.R., Hilgen, F.J., Sierro, F.J., 2001. Astrochronology for the Messinian Sorbas basin (SE Spain) and orbital (precessional) forcing for evaporite cyclicity. Sedimentary Geology 140, 43–60.
Legendre, S., Bachelet, B., 1993. The numerical ages; a new method of datation applied to Paleogene mammalian localities from Southern France. Newsletters of Stratigraphy 29, 137–158.
Mansino, S., Fierro, I., Tosal, A., Montoya, P., Ruiz-Sánchez, F.J., 2017. Micromammal biostratigraphy of the Alcoi Basin (eastern Spain): remarks on the Pliocene record of the Iberian Peninsula. Geologica Acta 15, 121–134.
Martín Suárez, E., Oms, O., Freudenthal, M., Agustí, J., Parés, J.M., 1998. Continental Mio-Pliocene transition in the Granada Basin. Lethaia 31, 161–166.
Martín-Suárez, E., Freudenthal, M., 1993. Muridae (Rodentia) from the Lower Turolian of Crevillente (Alicante, Spain). Scripta Geologica 103, 65–118.
Martín-Suárez, E., Freudenthal, M., 1998. Biostratigraphy of the continental upper Miocene of Crevillente (Alicante, SE Spain). Geobios 31, 839–847.
Martín-Suárez, E., Mein, P., 1998. Revision of the genera *Parapodemus*, *Apodemus*, *Rhagamys* and *Rhagapodemus* (Rodentia, Mammalia). Geobios 31, 87–97.
Martín-Suárez, E., Freudenthal, M., Krijgsman, W., Rutger, F.A., 2000. On the age of the continental deposits of the Zorreras Member (Sorbas Basin, SE Spain). Geobios 33, 505–512.
Maul, L.C., Masini, F., Abbazzi, L., Turner, A., 1998. Geochronometric application of evolutionary trends in the dentition of fossil Arvicolidae. In: van Kolfschoten, T., Gibbard, P.L. (Eds.), The dawn of the Quaternary; proceedings of the SEQS-EuroMam symposium 1996. Nederlands Instituut voor Toegepaste Geowetenschappen TNO, Haarlem, Netherlands, pp. 565–572.
Maul, L.C., Markova, A.K., 2007. Similarity and regional differences in Quaternary arvicolid evolution in Central and Eastern Europe. Quaternary International 160, 81–99.
Mein, P., Moissenet, E., Truc, G., 1978. Les formations continentales du Néogène Supérieur des Vallées du Júcar et du Cabriel au NE d'Albacete (Espagne), biostratigraphie et environnement. Documents des Laboratoires de Géologie de la Faculté des Sciences de Lyon 72, 99–147.
Mein, P., Moissenet, E., Adrover, R., 1983. L'extension et l'âge des formations continentales pliocènes du fossé de Teruel (Espagne). Comptes-Rendus des Séances de l'Académie des Sciences, Serie 2 (296), 1603–1610.
Mein, P., Moissenet, E., Adrover, R., 1990. Biostratigraphie du Néogène supérieur du bassin de Teruel. Paleontologia i Evolució 23, 121–139.
Mein, P., 1989. Updating of MN zones. In: Lindsay, E., Fahlbusch, V., Mein, P. (Eds.), European Neogene mammal chronology. NATO ASI Series A, pp. 73–90.
Minwer-Barakat, R., García-Alix, A., Suarez, E.M., Freudenthal, M., Viseras, C., 2012. Micromammal biostratigraphy of the Upper Miocene to lowest Pleistocene continental deposits of the Guadix basin, southern Spain. Lethaia 45, 594–614.

Morales, J., Peláez-Campomanes, P., Abella, J., Montoya, P., Gibert, L., Scott, G., Cantalapiedra, J.L., Sanisidro, O., 2013. The Ventian mammal age (Latest Miocene): present state. Spanish Journal of Palaeontology 28, 149–160.
Nobel, F.A., Andriessen, P.A.M., Hebeda, E.H., Priem, H.N.A., Rondeel, H.E., 1981. Isotopic dating of the post-alpine Neogene volcanism in the Betic Cordilleras, Southern Spain. Geologie en Mijnbouw 60, 209–214.
Oms, O., Dinares-Turell, J., Agustí, J., Parés, J.M., 1999. Refinements of the European mammal biochronology from the magnetic polarity record of the Plio-Pleistocene Zújar section, Guadix-Baza basin, SE Spain. Quaternary Research 51, 94–103.
Oms, O., Agustí, J., Gabas, M., Anadón, P., 2000. Lithostratigraphical and correlation of micromammal sites and biostratigraphy of the upper Pliocene to lower Pleistocene in the Northeast Guadix-Baza Basin (southern Spain). Journal of Quaternary Science 15, 43–50.
Opdyke, N., Mein, P., Lindsay, E., Pérez-Gonzáles, A., Moissenet, E., Norton, V.L., 1997. Continental deposits, magnetostratigraphy and vertebrate paleontology, late Neogene of Eastern Spain. Palaeogeography, Palaeoclimatology, Palaeoecology 133, 129–148.
Padial-Ojeda, J., 1986. Estudio de los roedores y lagomorfos del Mioceno continental de la depresión de Granada. Tesis Doctoral, Universidad de Granada 303.
Opdyke, N., Mein, P., Moissenet, E., Pérez-González, A., Lindsay, E., Petko, M., 1989. The magnetic stratigraphy of the Late Miocene sediments of the Cabriel Basin, Spain. In: Lindsay, E., Fahlbusch, V., Mein, P. (Eds.), European Neogene mammal chronology. ASI Series A, NATO, pp. 507–514.
Piñero, P., Agustí, J., 2019. The rodent succession in the Sifón de Librilla section (Fortuna Basin, SE Spain): implications for the Mio-Pliocene boundary in the Mediterranean terrestrial record. Historical Biology 31, 279–321.
Piñero, P., Agustí, J., Oms, O., 2018. The late Neogene rodent succession of the Guadix-Baza basin (south-eastern Spain) and its magnetostratigraphic correlation. Palaeontology 61, 253–272.
Piñero, P., Verzi, D.H., 2020. A new early Pliocene murine rodent from the Iberian Peninsula and its biostratigraphic implications. Acta Palaeontologica Polonica 65, 719–731.
Pueyo, E.L., Muñoz, A., Laplana, C., Parés, J.M., 2016. The Last Appearance Datum of Hipparion in Western Europe: magnetostratigraphy along the Pliocene–Pleistocene boundary in the Villarroya Basin (Northern Spain). International Journal of Earth Sciences (Geologische Rundschau) 105, 2203–2220.
Raffi, I., Wade, B.S., Pälike, H., 2020. The Neogene Period. In: Gradstein, F.M., Ogg, J. G., Schmitz, M.D., Ogg, G. (Eds.), Geologic time scale 2020. Elsevier, Amsterdam, pp. 1141–1215.
Raup, D.M., 1991. A Kill Curve for Phanerozoic marine species. Paleobiology 17, 37–48.
Repenning, C.A., Fejfar, O., Heinrich, W.D., 1990. Arvicolid rodent biochronology of the Northern Hemisphere. In: Fejfar, O., Heinrich Wolf, D. (Eds.), International symposium on Evolution, phylogeny and biostratigraphy of arvicolids (Rodentia, Mammalia). Geological Survey, Prague, pp. 385–418.
Rümke, C.G., 1985. A review of fossil and Recent Desmaninae (Talpidae, Insectivora). Utrecht Micropaleontological Bulletins. Special Publication 4, 1–241.
Salvador, A., 1994. International Stratigraphic Guide. A guide to stratigraphic classification, terminology, and procedure. The Geological Society of America, Boulder.
Schmidt-Kittler, N., 1995. The vertebrate locality Maramena (Macedonia, Greece) at the Turolian-Ruscinian boundary (Neogene), Münchner Geowissenschaftliche Abhandlungen 28. Pfeil, Munich.
Scott, G.R., Gibert, L., Gibert, J., 2007. Magnetostratigraphy of the Orce Region (Baza Basin), SE Spain: New chronologies for Early Pleistocene faunas and hominid occupation sites. Quaternary Science Reviews 26, 415–435.
Tesakov, A.S., 1998. Voles of the Tegelen fauna. In: van Kolfschoten, T., Gibbard, P.L. (Eds.), The dawn of the Quaternary; proceedings of the SEQS-EuroMam symposium 1996. Nederlands Instituut voor Toegepaste Geowetenschappen TNO, Haarlem, Netherlands, pp. 71–134.
van Balen, R.T., Forzoni, A., van Dam, J.A., 2015. Active faulting and folding along Jumilla Fault Zone, northeastern Betics, Spain. Geomorphology 237, 88–97.
van Dam, J.A., 1997. The small mammals from the upper Miocene of the Teruel-Alfambra region (Spain): paleobiology and paleoclimatic reconstructions. Geologica Ultraiectina 156, 1–204.
van Dam, J.A., 2003. European mammal-based chronological systems: past, present and future. Deinsia 10, 85–96.
van Dam, J.A., 2004. Anourosoricini (Mammalia: Soricidae) from the Mediterranean region: a pre-Quaternary example of recurrent climate-controlled north-south range shifting. Journal of Paleontology 78, 741–764.
van Dam, J.A., Alcalá, L., Alonzo Zarza, A., Calvo, J.P., Garcés, M., Krijgsman, W., 2001. The upper Miocene mammal record from the Teruel-Alfambra region (Spain). The MN system and continental stage/age concepts discussed. Journal of Vertebrate Paleontology 21, 367–385.
van Dam, J.A., Abdul Aziz, H., Álvarez Sierra, M.Á., Hilgen, F.J., van den Hoek Ostende, L.W., Lourens, L.J., Mein, P., van der Meulen, A.J., Peláez-Campomanes, P., 2006. Long-period astronomical forcing of mammal turnover. Nature 443, 687–691.
van Dam, J.A., Furió, M., van Balen, R.T., 2014. Re-interpreting the biochronology of the La Celia and Los Gargantones mammal sites (Late Miocene, Murcia, Spain). Geobios 47, 155–164.
van de Weerd, A., 1976. Rodent fauna of the Mio-Pliocene continental sediments of the Teruel-Alfambra region, Spain. Utrecht Micropaleontological Bulletins. Special publication 2, 1–185.
van der Meulen, A.J., García-Paredes, I., Álvarez-Sierra, M.A., van Den Hoek Ostende, L.W., Hordijk, K., Oliver, A., Peláez-Campomanes, P., 2012. Updated Aragonian biostratigraphy: Small mammal distribution and its implications for the Miocene European chronology. Geologica Acta 10, 159–179.